Accepted Manuscript

Design, synthesis and biological evaluation of novel 2,3,4,9-tetrahydro-1*H*-pyrido[3,4-*b*]indole triazole derivatives as potent TRPV1 antagonists

Jinyu Li, Cunbin Nie, Yue Qiao, Jing Hu, Qifei Li, Qiang Wang, Xiaohui Pu, Lin Yan, Hai Qian

PII: S0223-5234(19)30524-0

DOI: https://doi.org/10.1016/j.ejmech.2019.06.007

Reference: EJMECH 11410

To appear in: *European Journal of Medicinal Chemistry*

Received Date: 29 March 2019

Revised Date: 3 June 2019

Accepted Date: 3 June 2019

Please cite this article as: J. Li, C. Nie, Y. Qiao, J. Hu, Q. Li, Q. Wang, X. Pu, L. Yan, H. Qian, Design, synthesis and biological evaluation of novel 2,3,4,9-tetrahydro-1*H*-pyrido[3,4-*b*]indole triazole derivatives as potent TRPV1 antagonists, *European Journal of Medicinal Chemistry* (2019), doi: https://doi.org/10.1016/j.ejmech.2019.06.007.

Design, synthesis and biological evaluation of novel 2,3,4,9-tetrahydro-1*H*-pyrido[3,4-b]indole triazole derivatives as potent TRPV1 antagonists

Jinyu Li[a], Cunbin Nie[a], Yue Qiao[a], Jing Hu[a], Qifei Li[b], Qiang Wang[c], Xiaohui Pu[a], Lin Yan[a*], Hai Qian[b*]

[a] Institute for innovative drug design and evaluation, School of Pharmacy, Henan University, N. Jinming Ave., Kaifeng, Henan, 475004, China

[b] State Key Laboratory of Natural Medicines, Center of Drug Discovery, China Pharmaceutical University, 24 Tongjiaxiang, Nanjing, Jiangsu, 210009, China

[c] School of pharmaceutical sciences, South-Central University For Nationalities, 182 Minyuan road, Wuhan, Hubei, 430074, China

Reported herein is the design, synthesis, and pharmacologic evaluation of a class of TRPV1 antagonists constructed on 2,3,4,9-tetrahydro-1*H*-pyrido[3,4-b]indole as A-region and triazole as B-region.

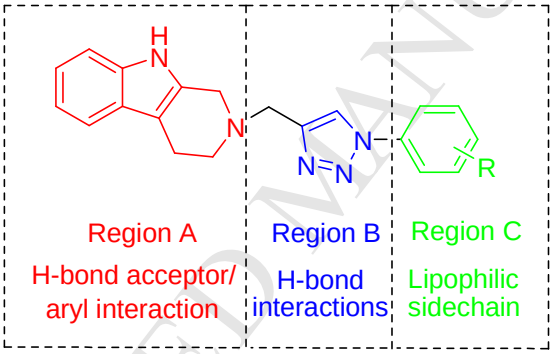

* Corresponding authors.

E-mail addresses: yanlin0378@163.com (L. Yan), qianhai24@163.com (H. Qian).

Design, synthesis and biological evaluation of novel 2,3,4,9-tetrahydro-1*H*-pyrido[3,4-b]indole triazole derivatives as potent TRPV1 antagonists

Jinyu Li[a], Cunbin Nie[a], Yue Qiao[a], Jing Hu[a], Qifei Li[b], Qiang Wang[c], Xiaohui Pu[a], Lin Yan[a*], Hai Qian[b*]

[a] Institute for innovative drug design and evaluation, School of Pharmacy, Henan University, N. Jinming Ave., Kaifeng, Henan, 475004, China

[b] State Key Laboratory of Natural Medicines, Center of Drug Discovery, China Pharmaceutical University, 24 Tongjiaxiang, Nanjing, Jiangsu, 210009, China

[c] School of pharmaceutical sciences, South-Central University For Nationalities, 182 Minyuan road, Wuhan, Hubei, 430074, China

ABSTRACT

Reported herein is the design, synthesis, and pharmacologic evaluation of a class of TRPV1 antagonists constructed on 2,3,4,9-tetrahydro-1*H*-pyrido[3,4-b]indole as A-region and triazole as B-region. The SAR analysis indicated that 2,3,4,9-tetrahydro-1*H*-pyrido[3,4-b]indole analogues displayed excellent antagonism of hTRPV1 activation by capsaicin and showed better potency compared to the corresponding dihydroindole analogues. Optimization of this design led to the eventual identification of 2-((1-(2-(trifluoromethyl)phenyl)-1*H*-1,2,3-triazol-4-yl)methyl)-2,3,4,9-tetrahydro-1*H*-pyrido[3,4-b]indole (**6g**), a potent TRPV1 antagonist. *In vitro*, using cells expressing recombinant human TRPV1 channels, **6g** displayed potent antagonism activated by capsaicin (IC_{50} = 0.075 μM) and only partially blocked acid activation of TRPV1. *In vivo*, **6g** exhibited good efficacy in capsaicin-induced and heat-induced pain models and had almost no hyperthermia side-effect. Furthermore, pharmacokinetic studies revealed that compound **6g** had a superior oral exposure after oral administration in rats. To understand its binding interactions with the receptor, the docking study of **6g** was performed in rTRPV1 model and showed an excellent fit to the binding site. On the basis of its superior profiles, **6g** could be considered as the lead candidate for the further development of antinociceptive drugs.

Keywords: Analgesic, Transient receptor potential vanilloid type 1, 2,3,4,9-tetrahydro-1*H*-pyrido[3,4-b]indole, 1,2,3-triazole, hyperthermia.

1. Introduction

TRPV1, the transient receptor potential vanilloid 1, is arguably the best-characterized member of the transient receptor potential (TRP) family: it is a calcium permeable nonselective ion channel gated by a wide range of stimuli such as exogenous ligands (e.g., capsaicin or resiniferatoxin), heat (>43 °C), acid (pH <6.8), and endogenous substances (e.g., anandamide and oxidative metabolites of linoleic acid), and is a central nociceptor on sensory afferent neurons[1-5].

* Corresponding authors.

E-mail addresses: yanlin0378@163.com (L. Yan), qianhai24@163.com (H. Qian).

Activation of this channel has been implicated in the pathophysiology of many neuronal (chronic inflammatory pain and peripheral neuropathy) and non-neuronal diseases, such as cystitis, asthma, and hearing loss [6, 7]. Therefore, TRPV1 antagonists have garnered great attention for the treatment of a variety of disease states, particularly in the management of pain physiology and neurogenic inflammation [8, 9]. To date, various structural classes of TRPV1 antagonists have been discovered, some of which have reached clinical trials, but none have advanced beyond due to their undesirable side effects such as hyperthermia that led to the termination of several drug development programs [10, 11]. Thus, pharmacological separation of analgesic and hyperthermic effects became the key challenge in developing TRPV1 antagonists as therapeutic agents for pain management. Recent reports have revealed that, complete blocking of all modes of TRPV1 activation (capsaicin, endogenous lipids, acidic pH, heat) in some models of chronic pain models can elicit hyperthermia [6, 12]. In addition, the magnitude and duration of the side effects seems to be different for different molecules. With distinct molecular domains for activation by capsaicin, protons, and heat, current intense interest exists to design modality-specific TRPV1 antagonists [13, 14]. Very recently, a number of diverse structures as modality-selective TRPV1 antagonists, which selectively inhibit capsaicin-induced TRPV1 activation but only partially block TRPV1 activation by acid, are recognized as the potential hyperthermia-free agents [6, 14, 15]. Taken together, these studies support the need for a different class of antagonists that can work in a particular activation mode, mainly by selectively blocking capsaicin-induced responses to avoid hyperthermia.

On the other hand, chemical modification of natural products or endogenous ligands, which can interfere with a given receptor, is a widely used strategy in medicinal chemistry programs [16]. Evodiamine and rutaecarpine are the two major components of *Evodia rutaecarpa*, which have been reported to possess multiple biological effects, such as antinociceptive, anti-inflammatory, antineoplastic, antidiabetic, and thermoregulatory effects, of which some are related to TRPV1 activity [17]. Furthermore, voacangine, a conformationally restricted tryptamine-derived natural product, is a stimulus-selective antagonist which competitively inhibits capsaicin binding to TRPV1 and blocks capsaicin- and heat-induced activation of this thermoreceptor [18]. These potent natural products share structural features (2,3,4,9-tetrahydro-1*H*-pyrido[3,4-b]indole group) that have been assumed to constitute a basic pharmacophore for TRPV1 blocking activity (Fig. 1). Therefore, we sought to design a series of new compounds containing 2,3,4,9-tetrahydro-1*H*-pyrido[3,4-b]indole group with improved modality-selective TRPV1 activation and pharmacodynamic profiles. Additionally, click chemistry, which commonly employs the 1,3-dipolar cycloaddition reaction between azides and alkynes to yield triazoles, has been widely applied in drug discovery as a rapid method to assemble compound libraries [19]. Further, triazoles are amphoteric in nature, acting as both acids and bases. Such properties make them usually soluble in aqueous medium. In order to rapidly generate a large number of diverse modality-selective TRPV1 antagonists with better physiochemical properties as potential drug candidates, we employed 1,3-dipolar azide-alkyne cycloaddition reaction to yield 1,4-disubstituted 1,2,3-triazoles. Herein, we report the design, synthesis, *in vitro* screening, and SAR analysis of a new family of TRPV1 antagonists built around a 2,3,4,9-tetrahydro-1*H*-pyrido[3,4-b]indole scaffold based on said pharmacophore (Fig. 2).

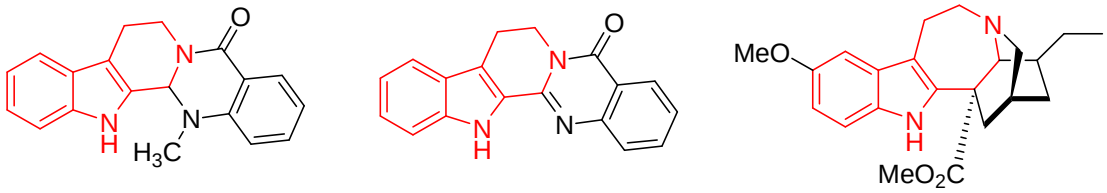

Fig. 1. Chemical structures of evodiamine, rutaecarpine, and voacangine used in this study.

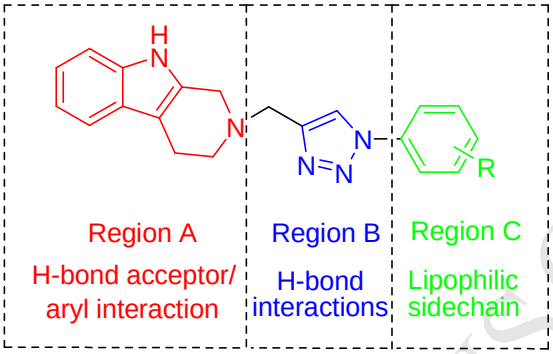

Fig. 2. Structure of the target TRPV1 antagonists.

2. Results and discussion

2.1. Chemistry

The work described in this paper stems from the observation that the pharmacophore of the TRPV1 antagonistic template can be divided into three regions: A, B and C (Fig. 2) [2]. The structure-activity relationship (SAR) of the template has been investigated in the most detail for the A-region, in which various functional groups including mono- or bicyclic-aryl and heteroaryl rings with a properly positioned hydrogen-bond receptor in this part of the molecule improving both potency and drug-like properties. In this study, a series of new TRPV1 antagonists were studied by using 2,3,4,9-tetrahydro-1*H*-pyrido[3,4-b]indole as the A-region of antagonistic template. Furthermore, we intended to explore whether the B-region such as urea, thiourea, amide could be isosterically replaced by the 1,4-disubstituted 1,2,3-triazole ring. For this purpose, the target compounds **6** were prepared according to Scheme 1. The starting material 2,3,4,9-tetrahydro-1*H*-pyrido[3,4-b]indole (**1**) was purchased directly. The synthetic protocol was straightforward enough to afford the two precursors in three steps: nucleophilic substitution, diazotation-azidation, and click reaction. Firstly, 2,3,4,9-tetrahydro-1*H*-pyrido[3,4-b]indole (**1**) was mixed with potassium carbonate in acetone, followed by addition of 3-bromo-1-propyne (**2**) and catalytic amount of potassium iodide to afford intermediate (**3**) in high yield. Secondly, a variety of aromatic amines (**4**) were diazotized by sodium nitrite to form diazonium salts, which were subsequently converted into azides (**5**). Lastly, the click reactions were performed under mild conditions. In general, compound **3** reacted with diverse azides (**5**) in the presence of copper sulfate and sodium ascorbate which guided the regioselectivity to obtain 1, 4-disubstituted 1,2,3-triazoles (**6**).

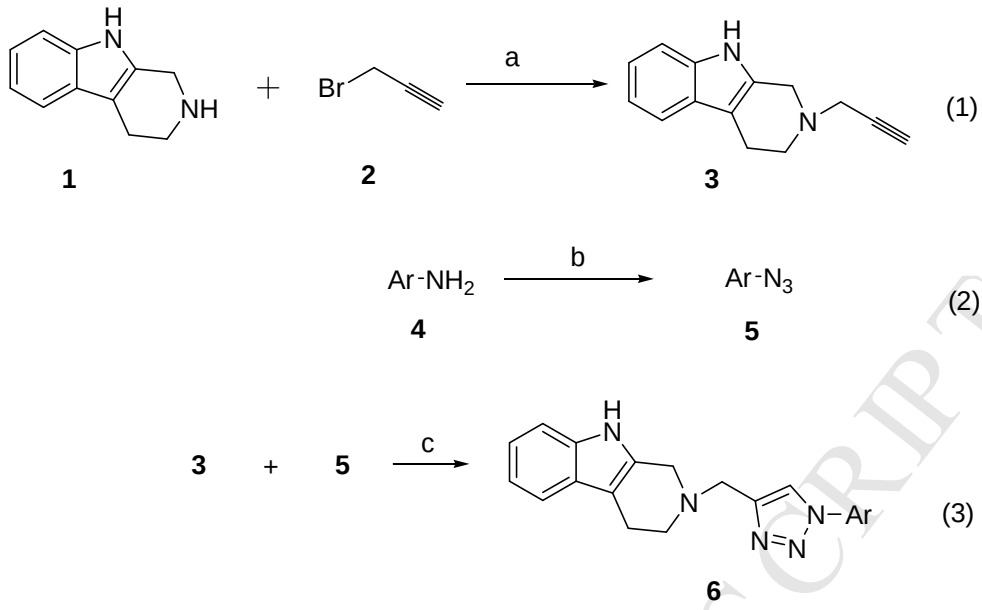

Scheme 1. Synthesis of the target compounds **6**. Reagents and conditions: (a) K_2CO_3, KI, acetone, rt; (b) $NaNO_2$, HCl, H_2O, 0-5 □, 30 min; NaN_3, 0-5 □, 2-4 h; (c) sodium ascorbate, $CuSO_4$, 75% CH_3OH, 24-48 h.

To probe the effect of 2,3,4,9-tetrahydro-1*H*-pyrido[3,4-b]indole on TRPV1 antagonism, a second series of products (**10**) were prepared starting from substituted indoles **7** in a similar way (Scheme 2). The synthesis of the dihydroindole-1,2,3-triazole derivatives was readily achieved by reduction of appropriately substituted indole using sodium cyanoborohydride, alkylation with 3-bromo-1-propyne (**2**) followed by a click reaction to afford compounds **10** according to the procedure as shown in Scheme 2.

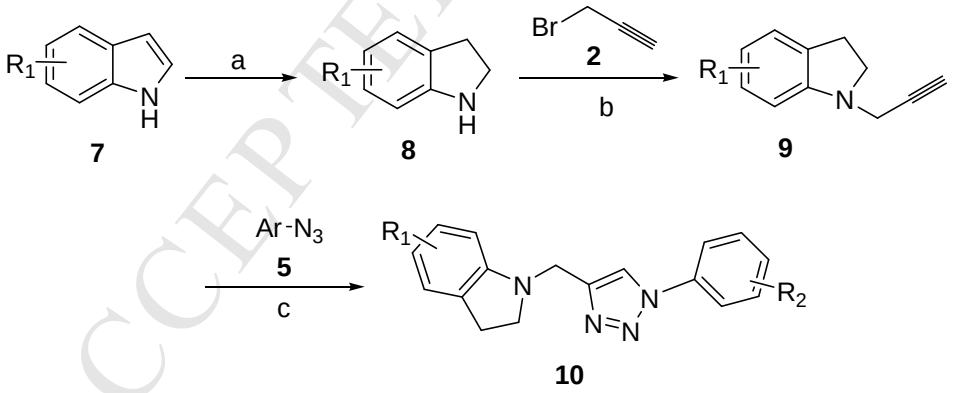

Scheme 2. Synthesis of the target compounds **10**. Reagents and conditions: (a) $NaCNBH_3$, acetic acid, rt; (b) K_2CO_3, KI, acetone, rt; (c) sodium ascorbate, $CuSO_4$, 75% CH_3OH, 24-48 h.

2.2. In vitro evaluation

With the obtained building blocks in hand, we initiated exploration of the SAR of the C-region aryl group (Table 1). The ability of these compounds to block capsaicin (CAP) or low pH-induced activation of human TRPV1 channels was assessed. As shown in Table 1, the phenyl **6A** showed potent competitive antagonism at recombinant human TRPV1 activated by capsaicin (IC_{50} = 0.314 μM) and incomplete blockade of acid-evoked response (68% block at 50 μM).

However, replacement of the phenyl group with two other types of aryl groups, isoquinoline (**6B**), pyridine (**6C** and **6D**) resulted in a significant loss of activity, indicating that C-region is important for the activity of this class of antagonists. Compound **6A** was selected for further optimization due to its potent TRPV1 antagonist potency against capsaicin activation. It was also noteworthy that compound **6A** exhibited different effects on capsaicin and pH 5.0 activation (only partially inhibited activation of the channel by protons).

Table 1

Effect of arene substitution on TRPV1 antagonism.

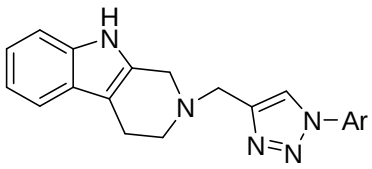

6

Compounds	Ar	hTRPV1(CAP) IC_{50} [a] (μM)	hTRPV1(pH) [b] % inhib @ 50 μM
6A	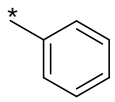	0.314 ± 0.087	68 ± 2
6B	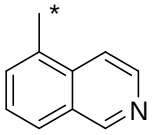	2.156 ± 0.323	59 ± 5
6C	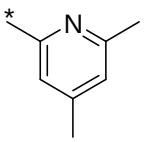	ND	13 ± 4
6D	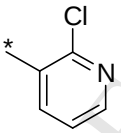	3.489 ± 0.278	72 ± 5

[a] Human TRPV1 receptor activated by capsaicin.

[b] Human TRPV1 receptor activated by low pH (5.0).

Unless otherwise stated, all values are the mean (SEM of at least three separate experiments).

ND, not determined.

Table 2

In vitro ability of compounds to inhibit the activation of hTRPV1 receptors.

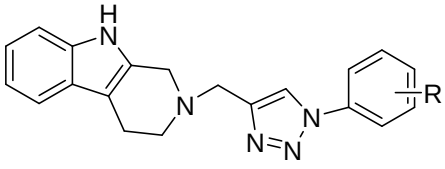

6

Compounds	R	hTRPV1(CAP) IC_{50}[a](μM)	hTRPV1(pH) [b] % inhib @ 50 μM
6a	2-Cl	0.243 ± 0.069	64 ± 5
6b	3-Cl	0.416 ± 0.094	71 ± 8
6c	4-Cl	0.495 ± 0.074	73 ± 2
6d	2-F	0.232 ± 0.069	57 ± 3
6e	3-F	0.385 ± 0.082	71 ± 8
6f	4-F	0.494 ± 0.032	74 ± 2
6g	2-CF_3	0.075 ± 0.029	58 ± 3
6h	3-CF_3	0.089 ± 0.057	62 ± 4
6i	4-CF_3	0.204 ± 0.043	79 ± 5
6j	2-NO_2	0.108 ± 0.071	85 ± 3
6k	2-*i*Pr	2.531 ± 0.055	67 ± 2
6l	2-OCH_3	1.878 ± 0.034	64 ± 3
6m	4-*t*Bu	1.217 ± 0.095	61 ± 7
6n	4-OCH_3	1.195 ± 0.038	55 ± 8
6o	4-NO_2	0.121 ± 0.047	86 ± 5
6p	4-Br	0.788 ± 0.049	78 ± 2
6q	3-*i*Pr	1.674 ± 0.032	40 ± 4
6r	2-NO_2, 4-CH_3	ND	71 ± 1
6s	2-NO_2, 4-Cl	0.394 ± 0.069	67 ± 7
6t	3-Cl, 4-CH_3	ND	48 ± 3
6u	3, 4-di-Cl	0.341 ± 0.052	73 ± 3
6v	2, 5-di-CH_3	1.543 ± 0.047	67 ± 2
6w	3, 4-di-OCH_3	1.122 ± 0.305	74 ± 6
6x	2, 5-di-Cl	0.112 ± 0.019	79 ± 5
6y	2, 4, 6-tri-CH_3	ND	13 ± 7
BCTC		0.019 ± 0.053	98 ± 1

[a] Human TRPV1 receptor activated by capsaicin.

[b] Human TRPV1 receptor activated by low pH (5.0).

Unless otherwise stated, all values are the mean (SEM of at least three separate experiments).

ND, not determined.

Next, as part of our continuing effort to optimize the C-region of our TRPV1 antagonistic template, we investigated the SAR of the substituted phenyl analogues. The results are presented in Table 2, together with the potency of the classical TRPV1 antagonist BCTC (*N*-(4-(tert-butyl)phenyl)-4-(3-chloropyridin-2-yl)piperazine-1-carboxamide). A variety of substituents such as the small lipophilic halogen group, alkyl, bulky group (*i*-propyl and *tert*-butyl), and even the multi-substituted benzene rings were investigated. An interesting trend has been observed through a deeper analysis of the SAR of the position of the substituent. In CAP assay, it was found that the *ortho*-substitution displayed higher potency than the *meta*-substitution or *para*-substitution. The representative examples include phenyls with chlorine (**6a** vs **6b**, **6c**), fluorine (**6d** vs **6e**, **6f**), and trifluoromethyl (**6g** vs **6h**, **6i**) substitutions (Table 2). Importantly, SAR studies demonstrated that the electron withdrawing groups such as fluorine, chlorine, trifluoromethyl and nitro-group were optimal. As illustrated in Table 2, 2-CF_3 analogue **6g** was the

most potent compound. Migrating the CF_3 group to the *meta* or *para* positions (**6h** and **6i**) reduced activity. The electron donating group substituent (e.g., **6k**) obviously decreased potency, as did a 2-OCH_3 group (**6l**). Moreover, introduction of the multisubstitution on the phenyl ring (**6r**, **6t** and **6y**) was poorly tolerated. However, in pH assay, in marked contrast to BCTC (a full blocker of acid activation), most of these analogues exhibited only partially blockade (<75%) of acid activation of TRPV1 at 50 μM. Interestingly, 2-CF_3 derivative **6g** exhibited differentiated effects on capsaicin (potent, competitive antagonism, IC_{50} = 0.075 μM) and pH 5.0 activation (incomplete blockade of acid-evoked response, 58% block at 50 μM) of recombinant human TRPV1.

Table 3

In vitro ability of compounds to inhibit the activation of hTRPV1 receptors.

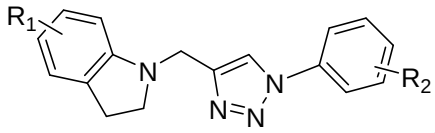

10

Compounds	R_1	R_2	hTRPV1(CAP) IC_{50}[a](μM)	hTRPV1(pH)[b] % inhib @ 50 μM
10a	H	4-*t*Bu	22.573 ± 1.386	32 ± 7
10b	H	3-F	19.416 ± 2.357	35 ± 6
10c	H	2-CF_3	4.945 ± 0.793	55 ± 3
10d	H	3-*i*Pr	ND	17 ± 6
10e	H	2-*i*Pr	ND	39 ± 7
10f	H	4-Cl	12.572 ± 4.653	42 ± 5
10g	5-Cl	4-Cl	ND	34 ± 8
10h	5-Cl	4-*t*Bu	27.071 ± 3.298	24 ± 4
10i	5-F	4-Cl	ND	12 ± 4

[a] Human TRPV1 receptor activated by capsaicin.

[b] Human TRPV1 receptor activated by low pH (5.0). Unless otherwise stated, all values are the mean (SEM of at least three separate experiments).

ND, not determined.

With the above result in hand, we further turned our investigation to the A-region of our TRPV1 antagonistic template, in order to assess the size of the substituents at the A-region and the effect of the 2,3,4,9-tetrahydro-1*H*-pyrido[3,4-b]indole group (Table 3). A second series of compounds (**10**) were synthesized (Scheme 2). Among these compounds, dihydroindole, which was also the nitrogen-containing heterocycle, was employed instead of 2,3,4,9-tetrahydro-1*H*-pyrido[3,4-b]indole. A range of substituents were introduced at the C-region phenyl moiety, including electron-withdrawing (F, Cl and CF_3) and electron-donating (*i*-propyl, and *tert*-butyl) groups. Intriguingly, with the size decreasing from three-ring to double-ring moiety, that is replacement of the 2,3,4,9-tetrahydro-1*H*-pyrido[3,4-b]indole group at A-region with dihydroindole resulted in drastic loss of activity. The most potent compound **10f** showed about a 65-fold loss of potency in CAP assay and slight loss of potency in pH assay compared to that of its parent compound **6g**. Furthermore, when the dihydroindole core was replaced by the substituted

dihydroindole, whereas chlorine and *tert*-butyl existed as substituents on the C-region phenyl moiety, it was found that this was not tolerated for *in vitro* potency. These findings implied that the 2,3,4,9-tetrahydro-1*H*-pyrido[3,4-b]indole group at the A-region was preferred.

2.3. In vivo evaluation

Based on the *in vitro* studies, five compounds (**6g**, **6h**, **6j**, **6o** and **6x**) were selected for further studies *in vivo*. In detail, the analgesic activity *in vivo* of each compound was evaluated employing three different models of pain (Fig. 3). A single oral dose of 30 mg/kg was administered to mice, as most of compounds were found to be almost not efficacious at 1 and 10 mg/kg in comparison with vehicle group. In the capsaicin test, the total time spent licking the paw was significantly reduced by all test compounds compared to the vehicle (Fig. 3A). Especially, compound **6g** exhibited greater potency than the positive control BCTC. In the abdominal constriction test, all compounds reduced the number of writhes in the proto-induced pain models and compounds **6j**, **6o** and **6x** exhibited better potency than BCTC (Fig. 3B). What is particularly interesting is that compound **6g,** the most active compound in the capsaicin test, had much weaker effect compared to other compounds, which was consistent with the activity observed in pH assay. In the tail-flick test, all compounds could increase %MPE compared to the vehicle. Compound **6g** exhibited a highest %MPE compared to other compounds in treatment of heat-induced pain, though it exhibited lowest analgesic activity in treatment of proton-induced pain (Fig. 3C). Overall, all the test compounds had antinociceptive activity to a certain extent. Among them, the most potent compound **6g** exhibited selective inhibitory activity in which it showed good antinociceptive potency in capsaicin- and heat-induced pain models, but displayed weak effect to low pH. Previous report indicated that hyperthermia depended on the blocking of TRPV1 activation by protons, suggesting that weak pH antagonism of **6g** was probably free of hyperthermia.

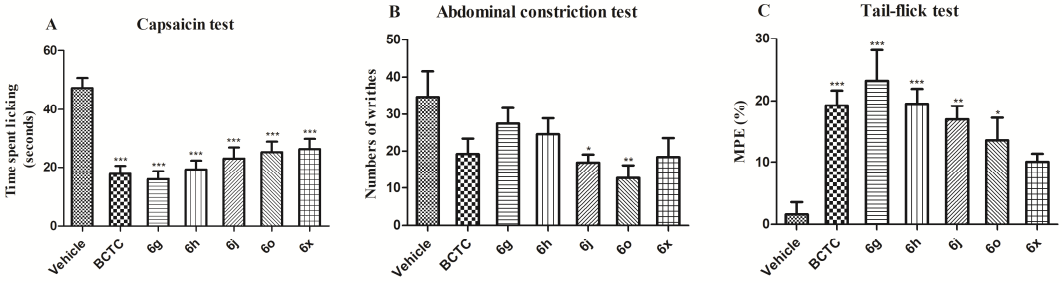

Fig. 3. Analgesic activities of synthesized compounds in 30 mg/kg after oral administration. (A) The antinociceptive effects in the capsaicin test; (B) suppression of acetic acid-induced writhing response; (C) inhibition of thermal nociception by synthesized compounds. Each bar represents the mean ± SEM (n = 6). Statistical analysis was evaluated using a one-way analysis of variance (ANOVA) followed by Dunnett's multiple comparison test. *p <0.05; **p <0.01; ***p <0.001 compared with the vehicle group.

We next conducted body temperature study and compared compounds effects with positive control BCTC (Fig. 4). A single oral dose of 30 mg/kg was administered to mice, and the core body temperature was measured every 30 min up to 120 min using a rectal thermometer. As shown in Fig. 4, BCTC displayed a significant increase in the core body temperature beginning 30 min after administration and lasting for at least 90 min. Similar to the effect of BCTC, compounds

6j, **6o** and **6x** also produced significant increase in the body temperature over vehicle-treated mice 30 min after administration, with a maximum of △ temperature occurring at 60 min. However, in contrast to BCTC, compounds **6g** and **6h,** which had the lipophilic substitution CF_3 group on C-region and exhibited weak effect in low pH-induced activation of human TRPV1 channel test, did not exhibit significant effects relative to vehicle. Furthermore, as previously mentioned in the three analgesic tests, **6g** was the most effective in treatment of capsaicin-induced and heat-induced pain, and not effective in proton-induced pain (Fig. 3). These results indicate that compound **6g** was the most promising compound and selected for further studies.

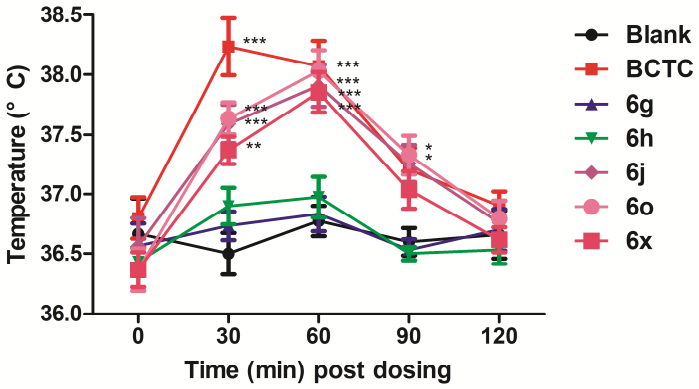

Fig. 4. The effects of compounds in 30 mg/kg after oral administration on body temperature in mice. Data are expressed as mean ± SEM (n = 6). *p < 0.05, **p < 0.01; ***p < 0.001 by Dunnett's multiple comparison test compared with the vehicle-treated group.

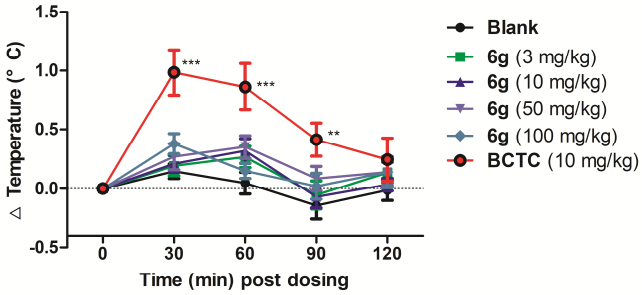

Fig. 5. The effects of compound **6g** at different doses on body temperature in mice. The changes of body temperature after dose. Data are expressed as mean ± SEM (n = 6). *p < 0.05, **p < 0.01; ***p < 0.001 by Dunnett's multiple comparison test compared with the vehicle-treated group.

To further explore the compound **6g**, the dose-dependency of increased core body temperature study were evaluated. More in detail, a single oral dose of **6g** (3, 10, 50, or 100 mg/kg) or BCTC (10 mg/kg) or vehicle was administered, and the core body temperatures were obtained at 30, 60, 90, and 120 min after dosing using a rectal thermometer. As illustrated in Fig. 5, **6g** slightly elevated the core body temperature above that of vehicle treated mice in a manner that was not clearly dose-dependent. Conversely BCTC, a potent blocker of both capsaicin and acid activation of TRPV1 *in vitro*, induced a robust increase in the core body temperature following a 10 mg/kg oral dose. In general, over all times and doses of **6g**, the average change of the core

body temperature was not significantly above vehicle and did not increase more than 0.53°C.

Following *in vitro* and *in vivo* studies, the most potent compound (**6g**) and its corresponding analogue (**6h**) were further assessed for their metabolic stability. The *in vivo* rat pharmacokinetic data which were analyzed using the one-compartment model for the compounds selected have been summarized in Table 4 and Fig. 6. As can be seen from Table 4, compound **6g** showed a favorable PK profile after a single oral administration of 10 mg/kg. Low clearance (CL 8.9 ± 1.1 L/h/kg) associated with moderate half-life ($t_{1/2}$ = 2.3 ± 0.7 h), high C_{max} (184.8 ± 53.4 ng/mL) and high AUC (1122 ± 229 ng/mL × h) was seen with **6g** oral administration. Compared to **6g**, compound **6h** has rapid absorption (T_{max} = 1.3 ± 0.3 h), but lower Cmax (122.7 ± 35.5 ng/mL), higher clearance (CL = 22.7 ± 2.8 L/h/kg) and lower AUC (441 ± 89 ng/mL × h). These results indicate that compound **6g** had a superior PK profile compared to compound **6h**, consistent with the activity observed in pH assay and the analgesic activity *in vivo*.

Table 4

Pharmacokinetic parameters of **6g** and **6h** following oral administration[a] to rats[b].

Parameters	Unit	Compound	
		6g	**6h**
$t_{1/2}$, ka	h	0.9 ± 0.3	0.9 ± 0.4
$t_{1/2}$, k_{10}	h	2.3 ± 0.7	0.9 ± 0.3
k_a	1/h	0.75 ± 0.11	0.77 ± 0.13
k_{10}	1/h	0.31 ± 0.06	0.75 ± 0.11
V	L/kg	29.1 ± 1.1	30.4 ± 1.8
CL	L/h/kg	8.9 ± 1.1	22.7 ± 2.8
T_{max}	h	2.0 ± 0.4	1.3 ± 0.3
C_{max}	ng/mL	184.8 ± 53.4	122.7 ± 35.5
AUC $_{0\text{-inf}}$	ng/mL*h	1122 ± 229	441 ± 89
MRT	h	4.61 ± 0.34	2.64 ± 0.19

[a] Compound was prepared in 0.5% sodium carboxymethyl cellulose and administered at 10 mg/kg.

[b] n = 3.

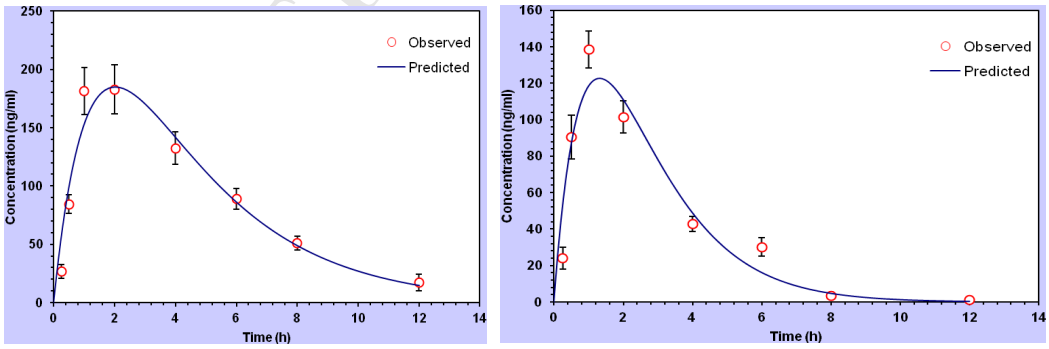

(A) (B)

Fig. 6. (A) Plasma concentrations in each time point of compound **6g** after intragastric gavage (10 mg/kg) in rats. (B) Plasma concentrations in each time point of compound **6h** after intragastric gavage (10 mg/kg) in rats. Each point is the average concentration, and the bars are standard deviations of the mean (n = 3).

2.4. Molecular modeling

In order to analyze the binding interactions of antagonist **6g** with the receptor, we carried out a docking study with rat TRPV1 (PDB ID: 5IS0) model [20] and compared its binding mode with that of BCTC.

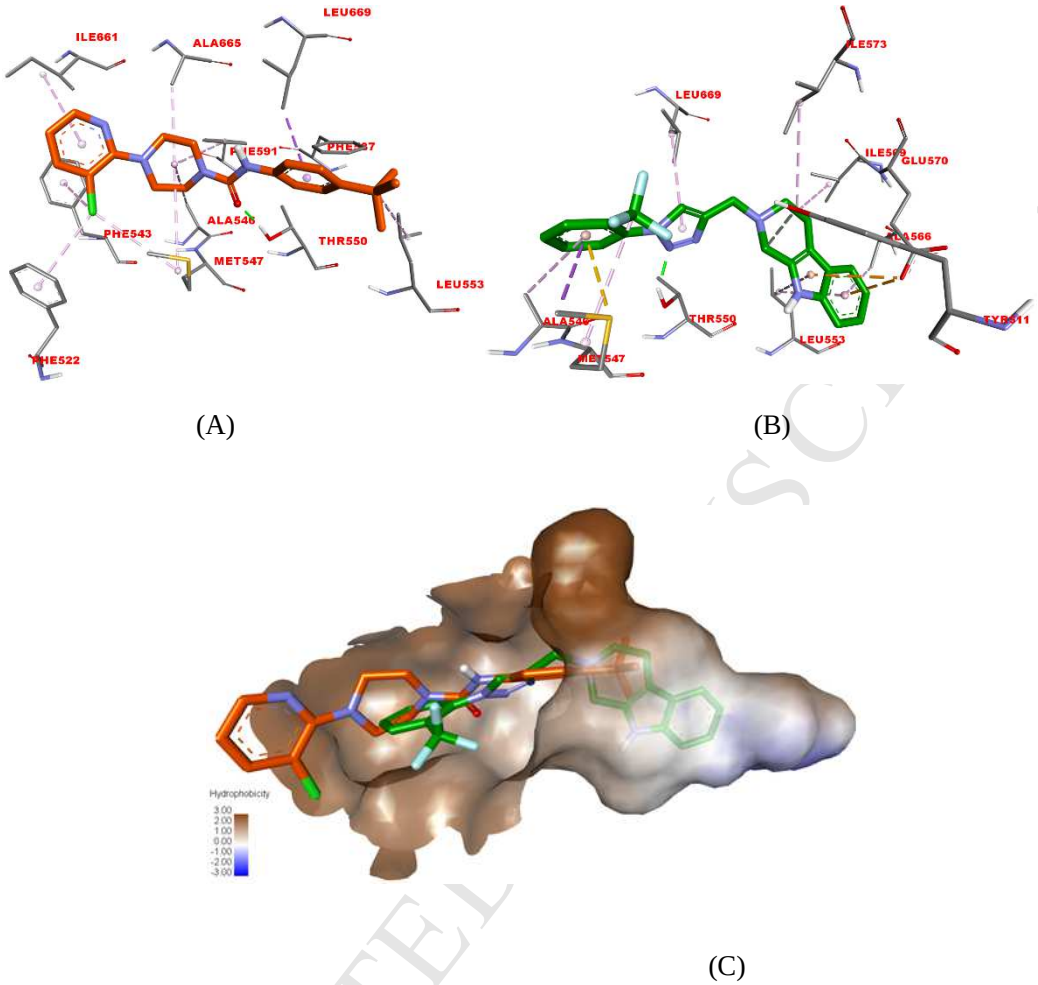

Fig. 7. Molecular modeling of compound **6g** and BCTC. (A) Three dimensional model of BCTC that interacts with the key amino acids of rTRPV1. (B) Three dimensional model of compound **6g** that interacts with the key amino acids of rTRPV1. (C) Three dimensional model of compounds in the hydrophobic pocket of rTRPV1. Compound **6g** is depicted by sticks colored by atom type (C dark green, F gray, N blue, polar H white). BCTC is depicted by sticks colored by atom type (C orange, O red, Cl green, N blue, polar H white).

As shown in Fig. 7A, an oxygen atom of the urea group of BCTC participated in hydrogen bonding with Thr550. The 4-*tert*-butylphenyl group was involved in a hydrophobic interaction with Leu553 and Leu669. Furthermore, the piperazine group made tight interactions with the binding site residues via the hydrophobic interaction with Ala665, Ala546, Phe591 and Met547. Additionally, the 3-chloropyridine group made an additional hydrophobic interaction with the hydrophobic region composed of Met547, Phe543, Phe522 and Ile661. As we expected, compound **6g** showed an excellent fit to the binding site (Fig. 7B). The 2,3,4,9-tetrahydro-1*H*-pyrido[3,4-b]indole (A-region) of compound **6g** made tight interactions with the binding site residues via the hydrogen bonding with Tyr511, electrostatic interaction with Glu570, and hydrophobic interaction with Leu553, Ala566, Ile569 and Ile573. Furthermore, the 1,2,3-triazole group (B-region) made a hydrogen bond with Thr550 and also contributed to the

hydrophobic interaction with Leu669. Moreover, the aromatic group in the C-region made an additional hydrophobic interaction with Ala546 and Met547. The 3-trifluoromethyl group in the C-region also formed a hydrophobic interaction with Met547, in addition to the hydrogen bonding with the 1,2,3-triazole group (B-region). Finally, as shown in Fig. 7C, compound **6g** fitted well into the active hydrophobic pocket better than BCTC. That might explain why the activity of **6g** was excellent.

3. Conclusions

In conclusion, we selected 2,3,4,9-tetrahydro-1*H*-pyrido[3,4-b]indole as the A-region, and a series of 1,2,3-triazole TRPV1 antagonists were newly designed and synthesized based on the click chemistry. Close scrutiny of our pharmacology data revealed compound **6g** was a potent TRPV1 antagonist that exhibited excellent *in vitro* functional activity and good efficacy in capsaicin-induced and heat-induced pain models. Consistent with its action *in vitro* being through TRPV1, compound **6g** blocked heat-induced and capsaicin-induced TRPV1 activation but did not cause TRPV1-related hyperthermia in mice. In addition, compound **6g** displayed promising pharmacokinetic properties in rats following oral administration. The docking study with the rTRPV1 model indicated that **6g** showed an excellent fit to the binding site resulting in its high potency. Taken together, this investigation has provided us with novel scaffolds for the further studies of related TRPV1 antagonists.

4. Experimental section

4.1. Biological methods

The synthesized compounds were investigated for TRPV1 antagonistic *in vitro*, *in vivo* analgesic activity and the effect on body temperature. The test compounds and the standard drugs were administered in the form of a suspension (using 0.5% sodium carboxymethyl cellulose as a vehicle) by intragastric administration. Separate groups of KM male mice (n = 6), weighing 18-22 g, were pretreated with compounds (30 mg/kg unless otherwise indicated) 30 min before the test. The animals were procured from the Comparative Medicine Centre of Yangzhou University (Jiangsu, China) and were maintained in colony cages at 25 ± 2 °C, relative humidity 45-55%, under a 12 h light/dark cycle; they were fed standard animal feed. All the animals were acclimatized for a week before use. The Institutional Animal Ethics committee has approved the protocol adopted for the experimentation of animals.

4.1.1. Transient receptor potential vanilloid type1 antagonistic activity assays in vitro

Culture plates with Ca^{2+}- and Mg^{2+}-free phosphate-buffered saline supplemented with 5 mM ethylenediaminetetra-acetic acid were used for the TRPV1 aequorin cells (Perkin Elmer, Waltham, MA, USA) growth. The cells were pelleted for 2 min at 1000 *g*; resuspended in Dulbecco's minimum essentialmedium-F12 medium with 15 mM HEPES (pH 7.0) and 0.1% BSA (assay buffer) at a density of 3×10^5 cells/mL and incubated for 4 h in the dark in the presence of 5 mM Coelenterazine (Promega, Madison, WI, USA). After loading, cells were diluted with assay buffer to a concentration of 5×10^6 cells/mL. Twenty microliter of cells was injected over 20 μL of the sample solution plated on 384-well plates, respectively, unless otherwise indicated. The Digitonin, ATP (Sigma-aldrich, St Louis, MO, USA), and assay buffer were added in the blank control wells for reference, and final concentration of Digitonin and ATP was100 and 50 μM. The sample

solution and the cells were incubated for 2.5 min before added agonists capsaicin (Tocris, England) and HCl solution at pH 5 and then immediately detected. The light emission was recorded during variable times using EnVision2014 Multilabel Reader (PerkinElmer) [21, 22].

4.1.2. Analgesic activity

4.1.2.1. Capsaicin test

As previously described, we evaluated analgesic activity in the capsaicin-induced pain model [23]. Twenty microliter of solution of capsaicin (16 μg/20 mL) was injected s.c. under the skin of the dorsal surface of the right hind paw. The mouse was then placed in an individual cage. The amount of time spent licking the injected paw was measured and expressed as the cumulative licking time for 5 min after the capsaicin injection.

4.1.2.2. Abdominal constriction test

Abdominal constriction test was performed as described previously to assess analgesia of pain activated by acid [24]. We placed mice in individual glass cylinders for a 30 min acclimatization period, injected with 0.6% acetic acid (0.1 mL/10 g/mouse i.p.), and immediately placed inside transparent glass cylinders. The number of writhes was recorded for 15 min.

4.1.2.3. Tail-flick test

Tail-flick test was carried out according to previous performation [24]. Briefly, in a water bath maintained at 52 °C, the distal one-third of the mouse tail was immersed. Latency times until a tail-flick response were recorded before and after drug treatment. The antinociception response was presented as percentmaximal possible effect (%MPE) as defined by %MPE = 100% × (drug response time - basal responsetime)/(cut-off time - basal response time). A cut-off time of 12 s was applied to avoid tissue damage.

4.1.3. Effect on body temperature

Mice were intragastric administered with synthesized compounds (30 mg/kg, i.g.), BCTC (30 mg/kg, i.g.), or an equal volume of vehicle. The body temperature of mice was monitored by the electric probe thermometer (MT-1C/F, Ruidien, Shenzhen, China) at 0, 30, 60, 90, and 120 min after dosing. The effect on body temperature was presented as temperature or △ temperature = the temperature at the certain time after dosing – the temperature at 0 min after dosing.

4.1.4. Pharmacokinetic Study.

The animal studies were performed according to committee approved procedures. Spragur-Dawley male rats, each weighing 220-250 g, were quarantined for 1 week before use. The animals were surgically implanted with a jugularvein cannula 1 day before treatment and were fasted overnight before treatment. The compound was given to the rats (n = 3) as oral (10 mg/kg) dose prepared in a mixture of dosing vehicles. The volume of the dosing solution given was adjusted according to the body weight recorded before the drug was administered. At specific time points (0.25, 0.5, 1, 2, 4, 6, 8, and 12 h), about 250-μL of blood sample was collected from the jugular vein and transferred into heparin-pretreated Eppendorf (EP) tubes. The blood samples were centrifuged at 8000 g (4 °C) for 10 min and the plasma was transferred into EP tubes and stored in -20 °C.

A 50-μL aliquot of plasma sample was subjected to the deproteinization using 200-μL acetonitrile. After 1-min vortex, the sample mixture was centrifuged at 12 000 *g* (4 °C) for 20 min. The resulting supernatant was collected and dried using Eppendorf Concentrator Plus (Hamburg, Germany). The dry residuals were re-dissolved in 100-μL of acetonitrile/water (50:50, v/v). After centrifugation (12 000 *g*, 15 min), a 5-μL aliquot of the supernatant was injected into a UPLC-QTOF/MS system (Waters, Milford, MA, USA). The plasma concentration data were analyzed with a standard one-compartmental method.

4.1.5. Statistical analysis of the data

Statistical analyses were performed using specific software (GRAPHPAD INSTAT version 5.00; GraphPad software, San Diego, CA, USA). Comparisons were analyzed using a one-way analysis of variance (ANOVA) followed by Dunnett's multiple comparison test, unless otherwise stated. $p < 0.05$ is regarded as statistically significant.

4.2. Chemistry

4.2.1. General

All reagents were purchased from Shanghai Chemical Reagent Company. Column chromatography was carried out on silica gel (200-300 mesh) and monitored by thin layer chromatography performed on GF/UV 254 plates and were visualized by using UV light at 365 and 254 nm. ^{1}H NMR spectra: BrukerAVANCE □ apparatus at 400 MHz, in $CDCl_3$ unless otherwise indicated; δ in ppm rel. to Me_4Si, J in Hz. ^{13}C NMR spectra: BrukerAVANCE □ apparatus at 100 MHz, in $CDCl_3$ unless otherwise indicated; δ in ppm rel. to Me_4Si. HRMS (high-resolution mass spectra) were taken with a Thermo QE spectrometer, in m/z.

General procedure for the preparation of 2-(prop-2-ynyl)-2,3,4,9-tetrahydro-1H-pyrido[3,4-b]indole (3). To a solution of 1,2,3,4-Tetrahydro-9*H*-pyrido[3,4-b]indole (**1**, 0.5g, 2.9 mmol) in acetone (30 mL) at room temperature, anhydrous K_2CO_3 (0.8g, 5.8 mmol) was added and then stirred for 45 min. To the above reaction mixture, the solution of bromopropyne (**2**, 0.34g, 2.9 mmol) in acetone (10 mL) with a catalytic amount of KI was added dropwise and then stirred at room temperature for 12-24 h. The mixture was filtered and the filtrate was evaporated and the crude product was purified by silica gel column chromatography to give the **3** (0.46 g, 75% yield) as a tan solid.

General procedure for the preparation of 5. Compound **4** (10 mmol) was dissolved in HCl (6 mol/mL, 10 mL) at 0 □. To the above reaction mixture, the solution of sodium nitrite (0.6 g, 8.5 mmol) in H_2O (25 mL) was added dropwise at -5 to 0 □ within 30 min. The solution was vigorously stirred at 0-5 □ for 30 min. Sodium azide (40 mmol) in H_2O (50 mL) was added dropwise into the reaction mixture at 0-5 □. The resulting solution was stirred at room temperature for 2-4 h followed by diluting with ice water (200 mL) and extracting with EtOAc (3 × 100 mL). The combined organic layer was washed with water (2 × 60 mL), saturated aqueous $NaHCO_3$ (2 × 60 mL) and brine (2 × 50 mL), dried over anhydrous Na_2SO_4, filtered and concentrated in vacuo to afford compound **5**. The residual crude product was used directly without purification.

General procedure for the preparation of 6. To the solution of compound **3** (1 mmol) and **5** (1 mmol) in 75% methanol (40 mL), sodium ascorbate (30 mg) and $CuSO_4$ (10 mg) were added successively. The reaction solution was stirred at room temperature for 24-48 h. After filtration, the solvent was evaporated and the crude product was purified by silica gel column chromatography to give the desire product with high purity.

2-((1-phenyl-1*H*-1,2,3-triazol-4-yl)methyl)-2,3,4,9-tetrahydro-1*H*-pyrido[3,4-b]indole (6A). $C_{20}H_{19}N_5$, brown yellow solid (95.7% yield), mp = 223.2-223.8 °C; ^{1}H NMR (DMSO, 400MHz): δ ppm 10.69 (s, 1H, NH), 8.79 (s, 1H, C=CH), 7.93 (d, 2H, *J* = 8.0 Hz, Ar-H), 7.59 (t, 2H, *J* = 10.0 Hz, Ar-H), 7.48 (t, 1H, *J* = 10.0 Hz, Ar-H), 7.36 (d, 1H, *J* = 8.0 Hz, Ar-H), 7.27 (d, 1H, *J* = 8 Hz, Ar-H), 7.03-6.91 (m, 2H, Ar-H), 3.94 (s, 2H, CH_2), 3.70 (s, 2H, CH_2), 2.88 (t, 2H, *J* = 8.0 Hz, CH_2), 2.72 (t, 2H, *J* = 8.0 Hz, CH_2); ^{13}C NMR (DMSO, 100MHz): δ ppm 145.5, 137.2, 136.3, 133.1, 130.3, 128.9, 127.1, 122.4, 120.7, 120.4, 118.7, 117.7, 111.3, 106.7, 52.2, 50.8, 50.0, 21.5; HRMS (ESI) calcd. for $C_{20}H_{20}N_5$ $[M+H]^+$ 330.1713, found 330.1712.

2-((1-(isoquinolin-5-yl)-1*H*-1,2,3-triazol-4-yl)methyl)-2,3,4,9-tetrahydro-1*H*-pyrido[3,4-b]indole (6B). $C_{23}H_{20}N_6$, brown yellow solid (92.7% yield), mp = 147.2-149.6 °C; ^{1}H NMR ($CDCl_3$, 400MHz): δ ppm 9.33 (s, 1H, NH), 8.70 (s, 1H, C=CH), 8.54 (s, 1H, Ar-H), 8.09 (d, 1H, *J* = 12.0 Hz, Ar-H), 7.91 (s, 1H, Ar-H), 7.73-7.63 (m, 2H, Ar-H), 7.54 (d, 1H, *J* = 8.0 Hz, Ar-H), 7.44 (d, 1H, *J* = 12.0 Hz, Ar-H), 7.24 (t, 1H, *J* = 8.0 Hz, Ar-H),7.10-7.01 (m, 2H, Ar-H), 4.05 (s, 2H, CH_2), 3.79 (s, 2H, CH_2), 3.02 (t, 2H, *J* = 6.0 Hz, CH_2), 2.86 (t, 2H, *J* = 6.0 Hz, CH_2); ^{13}C NMR ($CDCl_3$, 100MHz): δ ppm 152.6, 145.0, 144.7, 136.2, 131.4, 130.7, 129.8, 128.9, 127.1, 126.6, 125.2, 121.3, 119.2, 117.9, 115.2, 110.8, 107.8, 53.4, 52.2, 51.0, 50.0, 21.3; HRMS (ESI) calcd. for $C_{23}H_{20}N_6$ $[M+H]^+$ 381.1822, found 381.1819.

2-((1-(4,6-dimethylpyridin-2-yl)-1*H*-1,2,3-triazol-4-yl)methyl)-2,3,4,9-tetrahydro-1*H*-pyrido[3,4-b]indole (6C). $C_{21}H_{22}N_6$, brown yellow solid (73.0% yield), mp = 176.6-178.2 °C; ^{1}H NMR ($CDCl_3$, 400MHz): δ ppm 11.63 (s, 1H, NH), 7.93 (s, 1H, C=CH), 7.39 (s, 1H, Ar-H), 7.36 (d, 1H, *J* = 12.0 Hz, Ar-H), 7.22 (d, 1H, *J* = 8.0 Hz, Ar-H), 7.03 (s, 1H, Ar-H), 6.94 (s, 1H, Ar-H), 6.91 (s, 1H, Ar-H), 3.67 (s, 2H, CH_2), 3.62 (s, 2H, CH_2), 2.83 (s, 2H, CH_2), 2.73 (s, 2H, CH_2) , 2.49 (s, 3H, CH_3) , 2.47 (s, 3H, CH_3); ^{13}C NMR ($CDCl_3$, 100MHz): δ ppm 158.4, 147.3, 140.0, 136.3, 131.4, 127.6, 126.7, 124.3, 121.6, 119.7, 117.8, 111.1, 106.0, 57.2, 55.8, 53.6, 24.3, 21.7, 20.7; HRMS (ESI) calcd. for $C_{21}H_{23}N_6$ $[M+H]^+$ 359.1979, found 359.1981.

2-((1-(2-chloropyridin-3-yl)-1*H*-1,2,3-triazol-4-yl)methyl)-2,3,4,9-tetrahydro-1*H*-pyrido[3,4-b]indole (6D). $C_{19}H_{17}ClN_6$, cyan solid (74.2% yield), mp = 155.4-157.3 °C; ^{1}H NMR ($CDCl_3$, 400MHz): δ ppm 10.65 (s, 1H, NH), 8.38 (s, 1H, C=CH), 8.31 (s, 1H, Ar-H), 8.07 (s, 1H, Ar-H), 7.66-7.21 (m, 3H, Ar-H), 6.97 (s, 1H, Ar-H), 6.94 (s, 1H, Ar-H), 3.65 (s, 2H, CH_2), 3.61 (s, 2H, CH_2), 2.83 (s, 2H, CH_2), 2.71 (s, 2H, CH_2); ^{13}C NMR ($CDCl_3$, 100MHz): δ ppm 149.7, 140.6, 139.2, 136.2, 132.8, 131.1, 127.3, 126.7, 122.3, 121.6, 119.8, 118.7, 118.1, 111.1, 107.0, 57.2, 55.4, 52.3, 20.7; HRMS (ESI) calcd. for $C_{19}H_{18}ClN_6$ $[M+H]^+$ 365.1276, found 365.1279.

2-((1-(2-chlorophenyl)-1*H*-1,2,3-triazol-4-yl)methyl)-2,3,4,9-tetrahydro-1*H*-pyrido[3,4-b]indole (6a). $C_{20}H_{18}ClN_5$, pale yellow solid (91.6% yield), mp = 143.6-145.0 °C; ^{1}H NMR

(DMSO, 400MHz): δ ppm 10.62 (s, 1H, NH), 8.42 (s, 1H, C=CH), 7.68 (d, 1H, *J* = 8.0 Hz, Ar-H), 7.62 (d, 1H, *J* = 12.0 Hz, Ar-H), 7.52 (t, 2H, *J* = 10.0 Hz, Ar-H), 7.27 (d, 1H, *J* = 8.0 Hz, Ar-H), 7.18 (t, 1H, *J* = 12.0 Hz, Ar-H), 6.94-6.82 (m, 2H, Ar-H), 3.87 (s, 2H, CH_2), 3.60 (s, 2H, CH_2), 2.79 (t, 2H, *J* = 8.0 Hz, CH_2), 2.65 (t, 2H, *J* = 14.0 Hz, CH_2); ^{13}C NMR (DMSO, 100MHz): δ ppm 143.7, 135.8, 134.6, 132.6, 131.5, 130.4, 128.5, 128.4, 128.3, 126.6, 126.0, 120.2, 118.2, 117.2, 110.8, 106.2, 51.6, 50.2, 49.3, 21.0; HRMS (ESI) calcd. for $C_{20}H_{19}ClN_5$ $[M+H]^+$ 364.1323, found 364.1319.

2-((1-(3-chlorophenyl)-1*H*-1,2,3-triazol-4-yl)methyl)-2,3,4,9-tetrahydro-1*H*-pyrido[3,4-b]indole (6b). $C_{20}H_{18}ClN_5$, brown yellow solid (87.4% yield), mp = 181.4-182.4 °C; ^{1}H NMR (DMSO, 400MHz): δ ppm 10.66 (s, 1H, NH), 8.85 (s, 1H, C=CH), 8.07 (s, 1H, Ar-H), 7.95 (d, 1H, *J* = 12.0 Hz, Ar-H), 7.64-7.52 (m, 2H, Ar-H), 7.36 (d, 1H, *J* = 8.0 Hz, Ar-H), 7.27 (d, 1H, *J* = 8.0 Hz, Ar-H), 7.03-6.91 (m, 2H, Ar-H), 3.94 (s, 2H, CH_2), 3.71 (s, 2H, CH_2), 2.88 (t, 2H, *J* = 6.0 Hz, CH_2), 2.73 (t, 2H, *J* = 6.0 Hz, CH_2); ^{13}C NMR (DMSO, 100MHz): δ ppm 145.7, 138.2, 136.3, 134.6, 133.0, 132.0, 128.7, 127.1, 122.6, 120.7, 120.1, 118.9, 118.7, 117.7, 111.3, 106.7, 52.2, 50.7, 50.0, 21.5; HRMS (ESI) calcd. for $C_{20}H_{19}ClN_5$ $[M+H]^+$ 364.1323, found 364.1320.

2-((1-(4-chlorophenyl)-1*H*-1,2,3-triazol-4-yl)methyl)-2,3,4,9-tetrahydro-1*H*-pyrido[3,4-b]indole (6c). $C_{20}H_{18}ClN_5$, pale yellow solid (97.2% yield), mp = 237.0-237.2 °C; ^{1}H NMR (DMSO, 400MHz): δ ppm 10.69 (s, 1H, NH), 8.82 (s, 1H, C=CH), 7.98 (d, 2H, *J* = 8.0 Hz, Ar-H), 7.66 (d, 2H, *J* = 8.0 Hz, Ar-H), 7.36 (d, 1H, *J* = 8.0 Hz, Ar-H), 7.27 (d, 1H, *J* = 8.0 Hz, Ar-H), 7.01 (t, 1H, *J* = 8.0 Hz, Ar-H), 6.94 (t, 1H, *J* = 8.0 Hz, Ar-H), 3.94 (s, 2H, CH_2), 3.70 (s, 2H, CH_2), 2.88 (t, 2H, *J* = 6.0 Hz, CH_2), 2.72 (t, 2H, *J* = 6.0 Hz, CH_2); ^{13}C NMR (DMSO, 100MHz): δ ppm 136.3, 136.0, 133.2, 130.2, 129.3, 127.1, 126.1, 123.0, 122.0, 120.7, 118.7, 117.7, 111.1, 106.7, 52.3, 50.8, 50.0, 47.0, 21.5; HRMS (ESI) calcd. for $C_{20}H_{19}ClN_5$ $[M+H]^+$ 364.1323, found 364.1320.

2-((1-(2-fluorophenyl)-1*H*-1,2,3-triazol-4-yl)methyl)-2,3,4,9-tetrahydro-1*H*-pyrido[3,4-b]indole (6d). $C_{20}H_{18}FN_5$, brown yellow solid (79.0% yield), mp = 209.4-209.6 °C; ^{1}H NMR (DMSO, 400MHz): δ ppm 10.72 (s, 1H, NH), 8.55 (s, 1H, C=CH), 7.86 (t, 1H, *J* = 10.0 Hz, Ar-H), 7.64-7.52 (m, 2H, Ar-H), 7.44 (t, 1H, *J* = 10.0 Hz, Ar-H), 7.36 (d, 1H, *J* = 8.0 Hz, Ar-H), 7.28 (d, 1H, *J* = 12.0 Hz, Ar-H), 7.04-6.91 (m, 2H, Ar-H), 3.96 (s, 2H, CH_2), 3.71 (s, 2H, CH_2), 2.88 (t, 2H, *J* = 8.0 Hz, CH_2), 2.72 (t, 2H, *J* = 8.0 Hz, CH_2); ^{13}C NMR (DMSO, 100MHz): δ ppm 144.9, 136.3, 133.0, 131.6, 127.1, 126.3, 126.0, 125.7, 125.4, 120.7, 118.7, 117.8, 117.7, 117.4, 111.3, 106.7, 52.0, 50.7, 49.9, 21.5; HRMS (ESI) calcd. for $C_{20}H_{19}FN_5$ $[M+H]^+$ 348.1619, found 348.1618.

2-((1-(3-fluorophenyl)-1*H*-1,2,3-triazol-4-yl)methyl)-2,3,4,9-tetrahydro-1*H*-pyrido[3,4-b]indole (6e). $C_{20}H_{18}FN_5$, brown yellow solid (92.4% yield), mp = 196.1-198.2 °C; ^{1}H NMR (DMSO, 400MHz): δ ppm 10.68 (s, 1H, NH), 8.86 (s, 1H, C=CH), 7.89-7.86 (m, 2H, Ar-H), 7.64 (d, 1H, Ar-H), 7.38-7.27 (m, 3H, Ar-H), 7.03-6.92 (m, 2H, Ar-H), 3.95 (s, 2H, CH_2), 3.71 (s, 2H, CH_2), 2.89 (s, 2H, CH_2), 2.73 (s, 2H, CH_2); ^{13}C NMR (DMSO, 100MHz): δ ppm 164.1, 161.7, 145.7, 136.3, 133.0, 132.3, 127.1, 122.6, 120.7, 118.7, 117.7, 116.2, 115.7, 111.3, 107.9, 106.7, 52.2, 50.8, 50.0, 21.5; HRMS (ESI) calcd. for $C_{20}H_{19}FN_5$ $[M+H]^+$ 348.1619, found 348.1618.

2-((1-(4-fluorophenyl)-1*H*-1,2,3-triazol-4-yl)methyl)-2,3,4,9-tetrahydro-1*H*-pyrido[3,4-b]

indole (6f). $C_{20}H_{18}FN_5$, pale yellow solid (83.2% yield), mp = 237.9-238.8 °C; ^{1}H NMR (DMSO, 400MHz): δ ppm 10.67 (s, 1H, NH), 8.78 (s, 1H, C=CH), 8.00-7.79 (m, 2H, Ar-H), 7.45 (t, 2H, *J* = 8.0 Hz, Ar-H), 7.36 (d, 1H, *J* = 8.0 Hz Ar-H), 7.27 (d, 1H, *J* = 8.0 Hz, Ar-H), 7.01 (t, 1H, *J* = 8.0 Hz, Ar-H), 6.94 (t, 1H, *J* = 8.0 Hz, Ar-H), 3.94 (s, 2H, CH_2), 3.70 (s, 2H, CH_2), 2.89 (t, 2H, *J* = 6.0 Hz, CH_2), 2.73 (t, 2H, *J* = 6.0 Hz, CH_2); ^{13}C NMR (DMSO, 100MHz): δ ppm 163.2, 160.7, 145.6, 136.3, 133.7, 133.1, 127.1, 122.7, 120.7, 118.7, 117.7, 117.2, 117.0, 111.3, 106.7, 60.2, 52.3, 50.8, 50.0, 21.5; HRMS (ESI) calcd. for $C_{20}H_{19}FN_5$ $[M+H]^+$ 348.1619, found 348.1617.

2-((1-(2-(trifluoromethyl)phenyl)-1*H*-1,2,3-triazol-4-yl)methyl)-2,3,4,9-tetrahydro-1*H*-pyrido[3,4-b]indole (6g). $C_{21}H_{18}F_3N_5$, brown yellow solid (80.0% yield), mp = 145.5-145.8 °C; ^{1}H NMR ($CDCl_3$, 400MHz): δ ppm 8.37 (s, 1H, NH), 7.84 (d, 2H, *J* = 8.0Hz, C=CH, Ar-H), 7.72-7.63 (m, 3H, Ar-H), 7.52 (d, 1H, *J* = 8.0 Hz, Ar-H), 7.43 (d, 1H, *J* = 8.0 Hz Ar-H), 7.10-7.02 (m, 2H, Ar-H), 4.02 (s, 2H, CH_2), 3.77 (s, 2H, CH_2), 2.97 (s, 2H, CH_2), 2.84 (s, 2H, CH_2); ^{13}C NMR ($CDCl_3$, 100MHz): δ ppm 136.1, 133.0, 130.4, 128.9, 127.3, 127.2, 127.1, 126.0, 124.0, 121.2, 119.2, 117.8, 110.8, 107.8, 60.4, 53.4, 31.4, 29.7, 22.6, 21.0, 14.1; HRMS (ESI) calcd. for $C_{21}H_{19}F_3N_5$ $[M+H]^+$ 398.1587, found 398.1582.

2-((1-(3-(trifluoromethyl)phenyl)-1*H*-1,2,3-triazol-4-yl)methyl)-2,3,4,9-tetrahydro-1*H*-pyrido[3,4-b]indole (6h). $C_{21}H_{18}F_3N_5$, pale yellow solid (86.7% yield), mp = 190.2-190.5 °C; ^{1}H NMR ($CDCl_3$, 400MHz): δ ppm 8.35 (s, 1H, NH), 8.00 (s, 2H, C=CH, Ar-H), 7.89 (d, 1H, *J* = 8.0 Hz, Ar-H), 7.70-7.61 (m, 2H, Ar-H), 7.45 (d, 1H, *J* = 8.0 Hz , Ar-H), 7.24 (s, 1H, Ar-H), 7.12-7.05 (m, 2H, Ar-H), 3.99 (s, 2H, CH_2), 3.72 (s, 2H, CH_2), 2.99 (t, 2H, *J* = 6.0Hz, CH_2), 2.85 (t, 2H, *J* = 6.0Hz, CH_2); ^{13}C NMR($CDCl_3$, 100MHz): δ ppm 146.0, 137.3, 136.1, 131.4, 130.5, 127.1, 125.3, 123.4, 121.3, 121.0, 119.3, 117.9, 117.3, 110.8, 107.9, 52.3, 51.0, 50.0, 21.3; HRMS (ESI) calcd. for $C_{21}H_{19}F_3N_5$ $[M+H]^+$ 398.1587, found 398.1585.

2-((1-(4-(trifluoromethyl)phenyl)-1*H*-1,2,3-triazol-4-yl)methyl)-2,3,4,9-tetrahydro-1*H*-pyrido[3,4-b]indole (6i). $C_{21}H_{18}F_3N_5$, yellow solid (83.7% yield), mp = 191.0-193.5 °C; ^{1}H NMR (DMSO, 400MHz): δ ppm 10.66 (s, 1H, NH), 8.92 (s, 1H, C=CH), 8.19 (d, 2H, *J* = 8.0 Hz, Ar-H), 7.97 (d, 2H, *J* = 12.0 Hz, Ar-H), 7.36 (d, 1H, *J* = 12.0 Hz, Ar-H), 7.27 (d, 1H, *J* = 8.0 Hz, Ar-H), 7.03-6.91 (m, 2H, Ar-H), 3.96 (s, 2H, CH_2), 3.71 (s, 2H, CH_2), 2.89 (t, 2H, *J* = 8.0 Hz, CH_2), 2.73 (t, 2H, *J* = 6.0 Hz, CH_2); ^{13}C NMR(DMSO, 100MHz): δ ppm 146.0, 139.9, 136.3, 133.0, 129.2, 128.8, 127.6, 127.1, 122.7, 120.8, 118.7, 117.7, 111.3, 106.7, 52.2, 50.7, 50.0, 21.5; HRMS (ESI) calcd. for $C_{21}H_{19}F_3N_5$ $[M+H]^+$ 398.1587, found 398.1585.

2-((1-(2-nitrophenyl)-1*H*-1,2,3-triazol-4-yl)methyl)-2,3,4,9-tetrahydro-1*H*-pyrido[3,4-b]indole (6j). $C_{20}H_{18}N_6O_2$, brown yellow solid (87.3% yield), mp = 169.0-169.7 °C; ^{1}H NMR (DMSO, 400MHz): δ ppm 9.84 (s, 1H, NH), 7.77 (s, 1H, C=CH), 7.34 (d, 1H, *J* = 12.0 Hz, Ar-H), 7.10-6.93 (m, 3H, Ar-H), 6.48 (d, 1H, *J* = 8.0 Hz, Ar-H), 6.39 (d, 1H, *J* = 12.0 Hz , Ar-H), 6.15-6.03 (m, 2H, Ar-H), 3.08 (s, 2H, CH_2), 2.81 (s, 2H, CH_2), 1.99 (t, 2H, *J* = 12.0 Hz, CH_2), 1.84 (t, 2H, *J* = 12.0 Hz, CH_2); ^{13}C NMR (DMSO, 100MHz): δ ppm 144.5, 144.0, 136.3, 134.8, 133.0, 131.4, 129.7, 127.9, 127.1, 125.9, 125.6, 120.7, 118.7, 117.7, 111.3, 106.7, 52.0, 50.6, 49.8, 21.57; HRMS (ESI) calcd. for $C_{20}H_{19}N_6O_2$ $[M+H]^+$ 375.1564, found 375.1563.

2-((1-(2-isopropylphenyl)-1*H*-1,2,3-triazol-4-yl)methyl)-2,3,4,9-tetrahydro-1*H*-pyrido[3,4-b]indole (6k). $C_{23}H_{25}N_5$, brown yellow solid (95.0% yield), mp = 186.2-187.4 °C; ^{1}H NMR (DMSO, 400MHz): δ ppm 10.73 (s, 1H, NH), 8.39 (s, 1H, C=CH), 8.33 (s, 2H, Ar-H), 7.58 (s, 2H, Ar-H), 7.37 (d, 2H, *J* = 4.0 Hz, Ar-H), 7.29 (d, 1H, *J* = 8.0 Hz, Ar-H), 7.04-6.03 (m, 2H, Ar-H), 3.97 (s, 2H, CH_2), 3.74 (s, 2H, CH_2), 3.42 (s, 2H, CH_2), 2.74 (s, 2H, CH_2), 1.14 (d, 6H, *J* = 8.0 Hz, CH_3); ^{13}C NMR (DMSO, 100MHz): δ ppm 144.6, 136.3, 135.6, 133.1, 130.8, 127.2, 127.0, 126.5, 120.7, 118.7, 117.8, 111.3, 106.7, 60.2, 52.2, 50.7, 49.9, 28.0, 23.9, 21.6, 21.2, 14.5; HRMS (ESI) calcd. for $C_{23}H_{26}N_5$ $[M+H]^+$ 372.2183, found 372.2178.

2-((1-(2-methoxyphenyl)-1*H*-1,2,3-triazol-4-yl)methyl)-2,3,4,9-tetrahydro-1*H*-pyrido[3,4-b]indole(6l). $C_{21}H_{21}N_5O$, pale yellow solid (86.6% yield), mp = 168.6-169.3 °C; ^{1}H NMR (DMSO, 400MHz): δ ppm 10.71 (s, 1H, NH), 8.38 (s, 1H, C=CH), 7.65 (d, 1H, *J* = 8.0 Hz, Ar-H), 7.52 (t, 1H, *J* = 12.0 Hz, Ar-H), 7.37 (d, 1H, *J* = 12.0 Hz, Ar-H), 7.29 (t, 2H, *J* = 10.0 Hz, Ar-H), 7.14 (t, 1H, *J* = 10.0 Hz, Ar-H), 7.04-6.92 (m, 2H, Ar-H), 3.94 (s, 2H, CH_2), 3.85 (s, 3H, OCH_3), 3.71 (s, 2H, CH_2), 2.89 (t, 2H, *J* = 8.0 Hz, CH_2), 2.72 (t, 2H, *J* = 8.0 Hz, CH_2); ^{13}C NMR (DMSO, 100MHz): δ *ppm* 152.0, 144.0, 136.3, 133.1, 131.0, 127.1, 126.3, 126.1, 126.0, 121.3, 120.7, 118.7, 117.8, 113.4, 111.3, 106.7, 56.5, 52.2, 50.8, 49.9, 21.5; HRMS (ESI) calcd. for $C_{21}H_{22}N_5O$ $[M+H]^+$ 360.1819, found 360.1814.

2-((1-(4-tert-butylphenyl)-1*H*-1,2,3-triazol-4-yl)methyl)-2,3,4,9-tetrahydro-1*H*-pyrido[3,4-b]indole (6m). $C_{24}H_{27}N_5$, brown yellow solid (83.5% yield), mp = 224.4-227.4 °C; ^{1}H NMR (DMSO, 400MHz): δ ppm 10.68 (s, 1H, NH), 8.73 (s, 1H, C=CH), 7.84 (d, 2H, *J* = 8.0 Hz, Ar-H), 7.59 (d, 2H, *J* = 8.0 Hz, Ar-H), 7.36 (d, 1H, *J* = 4.0 Hz, Ar-H), 7.28 (d, 1H, *J* = 8.0 Hz, Ar-H), 7.01 (t, 1H, *J* = 8.0 Hz, Ar-H), 6.94 (t, 1H, *J* = 6.0 Hz, Ar-H), 3.94 (s, 2H, CH_2), 3.71 (s, 2H, CH_2), 2.89 (t, 2H, *J* = 4.0 Hz, CH_2), 2.73 (t, 2H, *J* = 6.0 Hz, CH_2), 1.32 (t, 9H, CH_3); ^{13}C NMR (DMSO, 100MHz): δ ppm 151.5, 145.4, 136.3, 134.9, 133.1, 127.1, 127.0, 122.3, 120.7, 120.1, 118.7, 117.7, 111.3, 106.7, 52.3, 50.8, 50.0, 34.92, 31.46, 21.56; HRMS (ESI) calcd. for $C_{24}H_{28}N_5$ $[M+H]^+$ 386.2339, found 386.2335.

2-((1-(4-methoxyphenyl)-1*H*-1,2,3-triazol-4-yl)methyl)-2,3,4,9-tetrahydro-1*H*-pyrido[3,4-b]indole (6n). $C_{21}H_{21}N_5O$, brown yellow solid (90.3% yield), mp = 216.7-219.7 °C; ^{1}H NMR (DMSO, 400MHz): δ ppm 10.69 (s, 1H, NH), 8.69 (s, 1H, C=CH), 7.84 (d, 2H, *J* = 12.0 Hz, Ar-H), 7.36 (d, 1H, *J* = 8.0 Hz, Ar-H), 7.27 (d, 1H, *J* = 12.0 Hz, Ar-H), 7.14 (d, 2H, *J* = 12.0 Hz, Ar-H), 7.03-6.91 (m, 2H, Ar-H), 3.92 (s, 2H, CH_2), 3.83 (s, 3H, OCH_3), 3.69 (s, 2H, CH_2), 2.88 (t, 2H, *J* = 8.0 Hz, CH_2), 2.72 (t, 2H, J = 8.0 Hz, CH_2); ^{13}C NMR (DMSO, 100MHz): δ ppm 159.5, 145.2, 136.3, 133.0, 130.6, 127.1, 122.4, 122.0, 120.7, 118.7, 117.8, 115.3, 111.3, 106.7, 56.0, 52.3, 50.8, 50.0, 21.5; HRMS (ESI) calcd. for $C_{21}H_{22}N_5O$ $[M+H]^+$ 360.1819, found 360.1817.

2-((1-(4-nitrophenyl)-1*H*-1,2,3-triazol-4-yl)methyl)-2,3,4,9-tetrahydro-1*H*-pyrido[3,4-b]indole (6o). $C_{20}H_{18}N_6O_2$, brown yellow solid (89.2% yield), mp = 201.4-202.5 °C; ^{1}H NMR (DMSO, 400MHz): δ ppm 10.65 (s, 1H, NH), 9.00 (s, 1H, C=CH), 8.44 (d, 2H, *J* = 12.0 Hz, Ar-H), 8.26 (t, 2H, *J* = 6.0 Hz, Ar-H), 7.36 (d, 1H, *J* = 8.0 Hz Ar-H), 7.26 (d, 1H, *J* = 6.0 Hz, Ar-H), 7.03-6.91 (m, 2H, Ar-H), 3.97 (s, 2H, CH_2), 3.71 (s, 2H, CH_2), 2.90 (t, 2H, *J* = 8.0 Hz, CH_2), 2.73 (t, 2H, *J* = 8.0 Hz, CH_2),; ^{13}C NMR (DMSO, 100MHz): δ ppm 170.7, 147.0, 146.2,

141.4, 136.3, 133.0, 127.1, 125.9, 122.9, 120.9, 118.7, 117.7, 111.3, 106.7, 60.2, 52.1, 50.7, 50.0, 21.1, 14.5; HRMS (ESI) calcd. for $C_{20}H_{19}N_6O_2$ $[M+H]^+$ 375.1564, found 375.1558.

2-((1-(4-bromophenyl)-1*H*-1,2,3-triazol-4-yl)methyl)-2,3,4,9-tetrahydro-1*H*-pyrido[3,4-b]indole (6p). $C_{20}H_{18}BrN_5$, brown yellow solid (87.2% yield), mp = 245.3-246.9 °C; ^{1}H NMR (DMSO, 400MHz): δ ppm 10.67 (s, 1H, NH), 8.82 (s, 1H, C=CH), 7.90 (s, 2H, Ar-H), 7.80 (s, 2H, Ar-H), 7.36 (d, 1H, *J* = 8.0 Hz, Ar-H), 7.28 (d, 1H, *J* = 8.0 Hz, Ar-H), 7.01 (t, 1H, *J* = 8.0 Hz, Ar-H), 6.95 (s, 1H, Ar-H), 3.94 (s, 2H, CH_2), 3.71 (s, 2H, CH_2), 2.89 (s, 2H, CH_2), 2.73 (s, 2H, CH_2); ^{13}C NMR (DMSO, 100MHz): δ ppm 145.6, 136.3, 133.2, 127.1, 122.5, 122.3, 121.5, 120.7, 118.7, 117.8, 111.3, 106.7, 52.5, 50.8, 50.0, 21.5; HRMS (ESI) calcd. for $C_{20}H_{19}BrN_5$ $[M+H]^+$ 408.0818, found 408.0817.

2-((1-(3-isopropylphenyl)-1*H*-1,2,3-triazol-4-yl)methyl)-2,3,4,9-tetrahydro-1*H*-pyrido[3,4-b]indole (6q). $C_{23}H_{25}N_5$, brown yellow solid (73.7% yield), mp = 167.0-168.9 °C; ^{1}H NMR ($CDCl_3$, 400MHz): δ ppm 8.57 (s, 1H, NH), 7.94 (s, 1H, C=CH), 7.56 (s, 1H, Ar-H), 7.45-7.36 (m, 3H, Ar-H), 7.26-7.21 (m, 1H, Ar-H), 7.05 (t, 2H, *J* = 12.0 Hz, Ar-H), 3.94 (s, 2H, CH_2), 3.68 (s, 2H, CH_2), 3.54 (s, 2H, CH_2), 2.82 (s, 2H, CH_2), 1.27 (d, 7H, *J* = 8.0 Hz, CH-CH_3); ^{13}C NMR ($CDCl_3$, 100MHz): δ ppm 151.0, 145.3, 137.0, 136.2, 131.6, 129.6, 127.1, 126.9, 121.2, 119.1, 118.7, 117.9, 110.9, 107.8, 53.4, 52.4, 50.9, 50.0, 34.1, 23.8, 21.3; HRMS (ESI) calcd. for $C_{23}H_{26}N_5$ $[M+H]^+$ 372.2183, found 372.2180.

2-((1-(4-methyl-2-nitrophenyl)-1*H*-1,2,3-triazol-4-yl)methyl)-2,3,4,9-tetrahydro-1*H*-pyrido[3,4-b]indole (6r). $C_{21}H_{20}N_6O_2$, brown yellow solid (92.0% yield), mp = 128.7-129.4 °C; ^{1}H NMR (DMSO, 400MHz): δ ppm 10.73 (s, 1H, NH), 8.60 (s, 1H, C=CH), 8.05 (d, 1H, *J* = 8.0 Hz, Ar-H), 7.74 (s, 2H, Ar-H), 7.37 (d, 1H, *J* = 8.0 Hz, Ar-H), 7.28 (d, 1H, *J* = 8.0 Hz, Ar-H), 7.02 (t, 1H, *J* = 8.0 Hz, Ar-H), 6.95 (t, 1H, *J* = 8.0 Hz, Ar-H), 3.97 (s, 2H, CH_2), 3.71 (s, 2H, CH_2), 2.89 (t, 2H, *J* = 6.0 Hz, CH_2), 2.74 (t, 2H, *J* = 6.0 Hz, CH_2), 2.50 (s, 3H, CH_3); ^{13}C NMR (DMSO, 100MHz): δ ppm 144.9, 144.3, 142.1, 136.3, 135.0, 133.1, 127.6, 127.4, 127.1, 125.9, 125.6, 120.7, 118.7, 117.8, 111.3, 106.7, 52.1, 50.7, 49.9, 21.6, 20.8; HRMS (ESI) calcd. for $C_{21}H_{21}N_6O_2$ $[M+H]^+$ 389.1721, found 389.1719.

2-((1-(4-chloro-2-nitrophenyl)-1*H*-1,2,3-triazol-4-yl)methyl)-2,3,4,9-tetrahydro-1*H*-pyrido[3,4-b]indole (6s). $C_{20}H_{17}ClN_6O_2$, brown yellow solid (88.0% yield), mp = 131.3-132.4 °C; ^{1}H NMR ($CDCl_3$, 400MHz): δ ppm 8.40 (s, 1H, NH), 8.00 (s, 1H, C=CH), 7.81 (s, 1H, Ar-H), 7.68 (d, 1H, *J* = 12.0 Hz, Ar-H), 7.42 (d, 2H, *J* = 8.0 Hz, Ar-H), 7.23 (d, 1H, *J* = 8.0 Hz, Ar-H), 7.11-7.02 (m, 2H, Ar-H), 4.00 (s, 2H, CH_2), 3.69 (s, 2H, CH_2), 2.98 (s, 2H, CH_2), 2.83 (s, 2H, CH_2); ^{13}C NMR ($CDCl_3$, 100MHz): δ ppm 144.4, 136.6, 136.1, 133.8, 128.8, 127.0, 125.7, 121.3, 119.2, 117.9, 110.8, 107.8, 60.4, 53.4, 52.1, 51.0, 49.7, 21.2, 21.0, 14.2; HRMS (ESI) calcd. for $C_{20}H_{18}ClN_6O_2$ $[M+H]^+$ 409.1174, found 409.1173.

2-((1-(3-chloro-4-methylphenyl)-1*H*-1,2,3-triazol-4-yl)methyl)-2,3,4,9-tetrahydro-1*H*-pyrido[3,4-b]indole (6t). $C_{21}H_{20}ClN_5$, brown yellow solid (90.3% yield), mp = 229.6-231.4 °C; ^{1}H NMR (DMSO, 400MHz): δ ppm 10.80 (s, 1H, NH), 8.96 (s, 1H, C=CH), 8.16 (s, 1H, Ar-H), 7.96 (d, 1H, *J* = 8.0 Hz, Ar-H), 7.67 (d, 1H, *J* = 8.0 Hz Ar-H), 7.47 (d, 1H, *J* = 8.0 Hz, Ar-H), 7.38 (d,

1H, *J* = 8.0 Hz , Ar-H), 7.12 (t, 1H, *J* = 8.0 Hz, Ar-H), 7.05 (t, 1H, *J* = 8.0 Hz, Ar-H), 4.05 (s, 2H, CH_2), 3.81 (s, 2H, CH_2), 3.48 (s, 3H, CH_3), 3.00 (s, 2H, CH_2), 2.84 (s, 2H, CH_3); ^{13}C NMR (DMSO, 100MHz): δ ppm 150.3, 141.0, 140.9, 140.8, 139.3, 137.4, 131.8, 125.5, 125.2, 123.6, 123.4, 122.5, 116.0, 111.4, 99.9, 57.0, 55.5, 54.7, 26.3, 24.4; HRMS (ESI) calcd. for $C_{21}H_{21}ClN_5$ $[M+H]^+$ 378.1480, found 378.1480.

2-((1-(3,4-dichlorophenyl)-1*H*-1,2,3-triazol-4-yl)methyl)-2,3,4,9-tetrahydro-1*H*-pyrido[3, 4-b]indole (6u). $C_{20}H_{17}Cl_2N_5$, brown yellow solid (84.0% yield), mp = 226.1-227.1 °C; ^{1}H NMR (DMSO, 400MHz): δ ppm 9.80 (s, 1H, NH), 8.02 (s, 1H, C=CH), 7.43 (d, 1H, *J* = 4.0 Hz, Ar-H), 7.12 (d, 1H, *J* = 12.0 Hz, Ar-H), 6.98 (d, 1H, *J* = 8.0 Hz, Ar-H), 6.48 (d, 1H, *J* = 8.0 Hz, Ar-H), 6.39 (d, 1H, *J* = 8.0 Hz, Ar-H), 6.13 (t, 1H, *J* = 8.0 Hz, Ar-H), 6.06 (t, 1H, *J* = 8.0 Hz, Ar-H), 3.07 (s, 2H, CH_2), 2.82 (s, 2H, CH_2), 2.01 (s, 2H, CH_2), 1.85 (s, 2H, CH_2); ^{13}C NMR (DMSO, 100MHz): δ ppm 150.6, 141.4, 141.0, 137.8, 137.5, 136.9, 135.9, 131.8, 127.4, 126.8, 125.5, 125.1, 123.4, 122.5, 116.0, 111.4, 57.0, 55.5, 54.7, 26.3; HRMS (ESI) calcd. for $C_{20}H_{18}Cl_2N_5$ $[M+H]^+$ 398.0934, found 398.0932.

2-((1-(2,5-dimethylphenyl)-1*H*-1,2,3-triazol-4-yl)methyl)-2,3,4,9-tetrahydro-1*H*-pyrido[3 ,4-b]indole (6v). $C_{22}H_{23}N_5$, brown yellow solid (81.0% yield), mp = 208.5-210.1 °C; ^{1}H NMR ($CDCl_3$, 400MHz): δ ppm 8.51 (s, 1H, NH), 7.69 (s, 1H, C=CH), 7.42 (d, 1H, *J* = 8.0 Hz, Ar-H), 7.22-7.17 (m, 3H, Ar-H), 7.14-7.01 (m, 3H, Ar-H), 3.98 (s, 2H, CH_2), 3.74 (s, 2H, CH_2), 2.96 (s, 2H, CH_2), 2.83 (s, 2H, CH_2), 2.34 (s, 3H, CH_3), 2.13 (s, 3H, CH_3); ^{13}C NMR ($CDCl_3$, 100MHz): δ ppm 136.8, 136.2, 131.2, 130.5, 130.1, 127.1, 126.4, 124.5, 121.2, 120.3, 120.2, 119.1, 117.8, 110.8, 107.8, 53.4, 52.3, 50.8, 50.2, 21.3, 20.7, 17.4; HRMS (ESI) calcd. for $C_{22}H_{24}N_5$ $[M+H]^+$ 358.2026, found 358.2025.

2-((1-(3,4-dimethoxyphenyl)-1*H*-1,2,3-triazol-4-yl)methyl)-2,3,4,9-tetrahydro-1*H*-pyrido [3,4-b]indole (6w). $C_{22}H_{23}N_5O_2$, brown yellow solid (87.1% yield), mp = 180.9-181.6 °C; ^{1}H NMR (DMSO, 400MHz): δ ppm 10.70 (s, 1H, NH), 8.75 (s, 1H, C=CH), 7.50-7.43 (m, 2H, Ar-H), 7.37 (d, 1H, *J* = 12.0 Hz, Ar-H), 7.27 (d, 1H, *J* = 8.0 Hz, Ar-H), 7.13 (d, 1H, *J* = 12.0 Hz, Ar-H), 7.04-6.91 (m, 2H, Ar-H), 3.94 (s, 2H, CH_2), 3.87 (s, 3H, CH_3), 3.82 (s, 3H, CH_3), 3.71 (s, 2H, CH_2), 2.91 (t, 2H, *J* = 6.0 Hz, CH_2), 2.74 (t, 2H, *J* = 6.0 Hz, CH_2); ^{13}C NMR (DMSO, 100MHz): δ ppm 149.7, 149.2, 145.1, 136.3, 132.9, 130.6, 127.1, 122.5, 120.8, 118.7, 117.8, 112.4, 111.3, 106.6, 104.9, 56.3, 56.2, 55.3, 52.3, 50.8, 50.0, 21.4; HRMS (ESI) calcd. for $C_{22}H_{24}N_5O_2$ $[M+H]^+$ 390.1925, found 390.1922.

2-((1-(2,5-dichlorophenyl)-1*H*-1,2,3-triazol-4-yl)methyl)-2,3,4,9-tetrahydro-1*H*-pyrido[3, 4-b]indole (6x). $C_{20}H_{17}Cl_2N_5$, pale yellow solid (88.0% yield), mp = 211.5-211.9 °C; ^{1}H NMR (DMSO, 400MHz): δ ppm 10.62 (s, 1H, NH), 8.45 (s, 1H, C=CH), 7.84 (s, 1H, Ar-H), 7.72 (d, 1H, *J* = 8.0 Hz, Ar-H), 7.64 (d, 1H, *J* = 4.0 Hz, Ar-H), 7.28 (d, 1H, *J* = 8.0 Hz, Ar-H), 7.19 (d, 1H, *J* = 8.0 Hz, Ar-H), 6.93 (t, 1H, *J* = 6.0 Hz, Ar-H), 6.86 (t, 1H, *J* = 8.0 Hz, Ar-H), 3.89 (s, 2H, CH_2), 3.63 (s, 2H, CH_2), 2.81 (t, 2H, *J* = 6.0 Hz, CH_2), 2.64 (t, 2H, *J* = 6.0 Hz, CH_2); ^{13}C NMR (DMSO, 100MHz): δ ppm 144.3, 136.3, 136.0, 133.0, 132.9, 132.3, 131.8, 128.6, 128.0, 127.1, 126.5, 120.7, 118.7, 117.7, 111.3, 106.7, 52.6, 50.7, 49.8, 21.5; HRMS (ESI) calcd. for $C_{20}H_{18}Cl_2N_5$ $[M+H]^+$ 398.0934, found 398.0931.

2-((1-mesityl-1*H*-1,2,3-triazol-4-yl)methyl)-2,3,4,9-tetrahydro-1*H*-pyrido[3,4-b]indole (6y). $C_{23}H_{25}N_5$, pale yellow solid (79.0% yield), mp = 148.5-149.9 °C; ^{1}H NMR ($CDCl_3$, 400MHz): δ ppm 8.56 (s, 1H, NH), 7.56 (s, 1H, C=CH), 7.44 (d, 1H, *J* = 8.0 Hz, Ar-H), 7.23 (s, 1H, *J* = 12.0 Hz, Ar-H), 7.10-7.02 (m, 2H, Ar-H), 6.98 (s, 2H, Ar-H), 4.03 (s, 2H, Ar-H), 3.73 (s, 2H, Ar-H), 2.95 (t, 2H, *J* = 8.0 Hz, CH_2), 2.84 (t, 2H, *J* = 8.0 Hz, CH_2), 2.35 (s, 3H, CH_3), 1.85 (s, 6H, CH_3); ^{13}C NMR ($CDCl_3$, 100MHz): δ ppm 144.1, 140.3, 136.2, 134.9, 133.5, 131.7, 129.1, 127.1, 124.9, 121.2, 119.1, 117.8, 110.8, 107.7, 60.4, 53.4, 52.3, 50.6, 49.8, 21.3, 21.1, 17.2, 14.2; HRMS (ESI) calcd. for $C_{23}H_{26}N_5$ $[M+H]^+$ 372.2183, found 372.2177.

General procedure for the preparation of 8. To a solution of compound **7** (1 mmol) in glacial acetic acid (10 mL) at room temperature, sodium cyanoborohydride (0.19 g, 3 mmol) was added. Then, the reaction was stirred at room temperature, monitored by TLC. Basification of the solution by $NaHCO_3$ (satd) was accomplished until pH value was about 8. The solution was extracted with CH_2Cl_2. The combined organic layers were dried by $MgSO_4$ and concentrated in vacuo to afford compound **8** for the next step without further purification.

General procedure for the preparation of 9. To a solution of compound **8** (2.9 mmol) in acetone (30 mL) at room temperature, anhydrous K_2CO_3 (0.8g, 5.8 mmol) was added and then stirred for 45 min. To the above reaction mixture, the solution of bromopropyne (**2**, 0.34g, 2.9 mmol) in acetone (10 mL) with a catalytic amount of KI was added dropwise and then stirred at room temperature for 12-24 h. The mixture was filtered and the filtrate was concentrated under vacuum to afford compound **9** for the next step without further purification.

General procedure for the preparation of 10. To the solution of compound **9** (1 mmol) and **5** (1 mmol) in 75% methanol (40 mL), sodium ascorbate (30 mg) and $CuSO_4$ (10 mg) were added successively. The reaction solution was stirred at room temperature for 24-48 h. After filtration, the solvent was evaporated and the crude product was purified by silica gel column chromatography to give the desire product with high purity.

1-((1-(4-tert-butylphenyl)-1*H*-1,2,3-triazol-4-yl)methyl)indoline (10a). $C_{21}H_{24}N_4$, brown yellow solid (85.9% yield), mp = 148.2-150.2 °C; ^{1}H NMR ($CDCl_3$, 400MHz): δ ppm 7.86 (s, 1H, C=CH), 7.60 (d, 2H, *J* = 8.0 Hz, Ar-H), 7.49 (d, 2H, *J* = 8.0 Hz, Ar-H), 7.08 (t, 2H, *J* = 10.0 Hz, Ar-H), 6.69 (t, 1H, *J* = 8.0 Hz, Ar-H), 6.60 (d, 1H, *J* = 4.0 Hz, Ar-H), 4.49 (s, 2H, CH_2), 3.43 (t, 2H, *J* = 8.0 Hz, CH_2), 2.96 (t, 2H, *J* = 8.0 Hz, CH_2), 1.34 (s, 9H, CH_3); ^{13}C NMR ($CDCl_3$, 100MHz): δ ppm 152.1, 151.6, 145.2, 134.5, 130.3, 127.3, 126.6, 126.3, 124.7, 120.2, 118.3, 115.0, 107.5, 53.5, 44.7, 34.8, 31.3, 28.6; HRMS (ESI) calcd. for $C_{21}H_{25}N_4$ $[M+H]^+$ 333.2074, found 333.2070.

1-((1-(3-fluorophenyl)-1*H*-1,2,3-triazol-4-yl)methyl)indoline (10b). $C_{17}H_{15}FN_4$, brown yellow solid (73.1% yield), mp = 143.8-146.2 °C; ^{1}H NMR ($CDCl_3$, 400MHz): δ ppm 7.86 (s, 1H, C=CH), 7.52-7.43 (m, 3H, Ar-H), 7.12-7.09 (m, 3H, Ar-H), 6.70 (t, 1H, *J* = 6.0 Hz, Ar-H), 6.59 (d, 1H, *J* = 8.0 Hz, Ar-H), 4.51 (s, 2H, CH_2), 3.45 (t, 2H, *J* = 8.0 Hz, CH_2), 2.98 (t, 2H, *J* = 8.0 Hz, CH_2); ^{13}C NMR ($CDCl_3$, 100MHz): δ ppm 151.5, 145.8, 138.1, 131.1, 130.3, 127.3, 124.7, 120.0,

118.3, 115.7, 108.3, 107.4, 44.7, 31.6, 28.5, 22.6, 14.1; HRMS (ESI) calcd. for $C_{17}H_{16}FN_4$ $[M+H]^+$ 295.1354, found 295.1352.

1-((1-(2-(trifluoromethyl)phenyl)-1*H*-1,2,3-triazol-4-yl)methyl)indoline (10c). $C_{18}H_{15}F_3N_4$, oily liquid (73.5% yield); ^{1}H NMR ($CDCl_3$, 400MHz): δ ppm 7.83 (s, 1H, C=CH), 7.72-7.63 (m, 3H, Ar-H), 7.53 (d, 1H, *J* = 8.0 Hz, Ar-H), 7.10-7.05 (m, 2H, Ar-H), 6.68 (t, 1H, *J* = 8.0 Hz, Ar-H), 6.61 (d, 1H, *J* = 8.0 Hz, Ar-H), 4.52 (s, 2H, CH_2), 3.41 (t, 2H, *J* = 8.0 Hz, CH_2), 2.96 (t, 2H, *J* = 10.0 Hz, CH_2); ^{13}C NMR ($CDCl_3$, 100MHz): δ ppm 151.6, 144.6, 134.8, 133.0, 131.3, 130.4, 130.3, 128.9, 127.3, 124.8, 124.6, 121.2, 118.3, 107.5, 53.4, 53.3, 44.6, 28.5; HRMS (ESI) calcd. for $C_{18}H_{16}F_3N_4$ $[M+H]^+$ 345.1322, found 345.1319.

1-((1-(3-isopropylphenyl)-1*H*-1,2,3-triazol-4-yl)methyl)indoline (10d). $C_{20}H_{22}N_4$, oily liquid (83.2% yield); ^{1}H NMR ($CDCl_3$, 400MHz): δ ppm 7.88 (s, 1H, C=CH), 7.60 (s, 1H, Ar-H), 7.47 (d, 1H, *J* = 8.0 Hz, Ar-H), 7.41 (t, 1H, *J* = 8.0 Hz, Ar-H), 7.29 (d, 1H, *J* = 8.0 Hz, Ar-H), 7.09 (t, 2H, *J* = 8.0 Hz, Ar-H), 6.70 (t, 1H, *J* = 8.0 Hz, Ar-H), 6.62 (d, 1H, *J* = 8.0 Hz, Ar-H), 4.51 (s, 2H, CH_2), 3.46 (t, 2H, *J* = 8.0 Hz, CH_2), 2.99 (t, 3H, *J* = 10.0 Hz, CH_2, C-CH), 1.30 (d, 6H, *J* = 4.0 Hz , CH_3); ^{13}C NMR ($CDCl_3$, 100MHz): δ ppm 151.6, 151.0, 145.4, 137.1, 130.3, 129.5, 127.3, 126.9, 124.6, 120.3, 118.8, 118.2, 117.9, 107.4, 53.5, 44.8, 34.1, 28.6, 23.8, 22.6; HRMS (ESI) calcd. for $C_{20}H_{23}N_4$ $[M+H]^+$ 319.1917, found 319.1914.

1-((1-(2-isopropylphenyl)-1*H*-1,2,3-triazol-4-yl)methyl)indoline (10e). $C_{20}H_{22}N_4$, oily liquid (85.1% yield); ^{1}H NMR ($CDCl_3$, 400MHz): δ ppm 7.61 (s, 1H, C=CH), 7.48 (t, 2H, *J* = 8.0 Hz, Ar-H), 7.32-7.28 (m, 1H, Ar-H), 7.25 (d, 1H, *J* = 8.0 Hz, Ar-H), 7.11-7.05 (m, 2H, Ar-H), 6.70 (t, 1H, *J* = 8.0 Hz, Ar-H), 6.62 (d, 1H, *J* = 8.0 Hz, Ar-H), 4.56 (s, 2H, Ar-H), 3.47 (t, 2H, *J* = 8.0 Hz, CH_2), 2.99 (t, 2H, *J* = 8.0 Hz, CH_2), 2.74-2.63 (m, 1H, C-CH), 1.16 (d, 6H, *J* = 8.0 Hz , CH_3); ^{13}C NMR ($CDCl_3$, 100MHz): δ ppm 151.6, 144.7, 144.4, 135.2, 130.4, 130.3, 127.3, 126.8, 126.5, 124.6, 124.3, 118.2, 107.6, 53.5, 44.7, 28.6, 27.9, 23.8, 22.2; HRMS (ESI) calcd. for $C_{20}H_{23}N_4$ $[M+H]^+$ 319.1917, found 319.1914.

1-((1-(4-chlorophenyl)-1*H*-1,2,3-triazol-4-yl)methyl)indoline (10f). $C_{17}H_{15}ClN_4$, oily liquid (89.6% yield); ^{1}H NMR ($CDCl_3$, 400MHz): δ ppm 7.86 (s, 1H, C=CH), 7.65 (d, 2H, *J* = 8.0 Hz, Ar-H), 7.46 (d, 2H, *J* = 8.0 Hz, Ar-H), 7.12-7.07 (m, 2H, Ar-H), 6.71 (t, 1H, *J* = 8.0 Hz, Ar-H), 6.60 (d, 1H, *J* = 8.0 Hz, Ar-H), 4.50 (s, 2H, CH_2), 3.45 (t, 2H, *J* = 8.0 Hz, CH_2), 2.98 (t, 2H, *J* = 8.0 Hz, CH_2); ^{13}C NMR ($CDCl_3$, 100MHz): δ ppm 151.5, 145.7, 135.5, 134.4, 130.3, 129.8, 127.3, 124.7, 121.6, 120.0, 118.3, 107.4, 53.5, 44.7, 28.6; HRMS (ESI) calcd. for $C_{17}H_{16}ClN_4$ $[M+H]^+$ 311.1058, found 311.1054.

5-chloro-1-((1-(4-chlorophenyl)-1*H*-1,2,3-triazol-4-yl)methyl)indoline (10g). $C_{17}H_{14}Cl_2N_4$, pale yellow solid (87.4% yield), mp = 137.0-138.5 °C; ^{1}H NMR ($CDCl_3$, 400MHz): δ ppm 7.85 (s, 1H, C=CH), 7.65 (d, 2H, *J* = 8.0 Hz, Ar-H), 7.46 (d, 2H, *J* = 8.0 Hz, Ar-H), 7.00 (d, 2H, *J* = 8.0 Hz, Ar-H), 6.48 (d, 1H, *J* = 8.0 Hz, Ar-H), 4.45 (s, 2H, CH_2), 3.46 (t, 2H, *J* = 8.0 Hz, CH_2), 2.94 (t, 2H, *J* = 8.0 Hz, CH_2); ^{13}C NMR ($CDCl_3$, 100MHz): δ ppm 150.2, 135.4, 134.4, 132.2, 129.8, 126.9, 124.8, 122.8, 121.5, 120.0, 107.9, 53.5, 44.4, 28.3, 22.6, 21.0, 14.2; HRMS (ESI) calcd. for $C_{17}H_{15}Cl_2N_4$ $[M+H]^+$ 345.0668, found 345.0665.

1-((1-(4-tert-butylphenyl)-1*H*-1,2,3-triazol-4-yl)methyl)-5-chloroindoline (10h) .$C_{21}H_{23}ClN_4$, brown yellow solid (73.6% yield), mp = 152.7-154.5 °C; ^{1}H NMR ($CDCl_3$, 400MHz): δ ppm 7.81 (s, 1H, C=CH), 7.61 (d, 2H, *J* = 8.0 Hz, Ar-H), 7.51 (d, 2H, *J* = 12.0 Hz, Ar-H), 7.02 (d, 2H, *J* = 8.0 Hz, Ar-H), 6.50 (d, 1H, *J* = 8.0 Hz, Ar-H), 4.47 (s, 2H, CH_2), 3.46 (t, 2H, *J* = 8.0 Hz, CH_2), 2.95 (t, 2H, *J* = 8.0 Hz, CH_2), 1.35 (s, 9H, CH_3); ^{13}C NMR ($CDCl_3$, 100MHz): δ ppm 152.1, 150.3, 144.7, 134.5, 132.2, 126.9, 126.6, 124.8, 122.7, 122.2, 120.4, 120.2, 108.0, 53.4, 44.5, 34.7, 31.2, 28.3; HRMS (ESI) calcd. for $C_{21}H_{24}ClN_4$ $[M+H]^+$ 367.1684, found 367.1682.

1-((1-(4-chlorophenyl)-1*H*-1,2,3-triazol-4-yl)methyl)-5-fluoroindoline (10i). $C_{17}H_{14}ClFN_4$, brown yellow solid (79.8% yield), mp = 119.2-122.1 °C; ^{1}H NMR ($CDCl_3$, 400MHz): δ ppm 7.86 (s, 1H, C=CH), 7.66 (d, 2H, *J* = 8.0 Hz, Ar-H), 7.47 (d, 2H, *J* = 8.0 Hz, Ar-H), 6.88-6.73 (m, 2H, Ar-H), 6.50-6.47 (m, 1H, Ar-H), 4.44 (s, 2H, CH_2), 3.43 (t, 2H, *J* = 8.0 Hz, CH_2), 2.94 (t, 2H, *J* = 8.0 Hz, CH_2); ^{13}C NMR ($CDCl_3$, 100MHz): δ ppm 157.9, 155.6, 147.8, 145.5, 135.4, 134.4, 132.0, 129.8, 121.5, 120.0, 113.1, 112.4, 107.6, 54.0, 45.3, 31.5, 28.6; HRMS (ESI) calcd. for $C_{17}H_{15}ClFN_4$ $[M+H]^+$ 329.0964, found 329.0960.

4.3. Docking experiments

Receptor protein (PDB ID: 5IS0) was prepared and optimized using relevant module by Sybyl-X 1.10 software. The 3D-interaction was plotted by Discovery Studio 4.1 Client.

Acknowledgment

This study was financially supported by the National Natural Science Foundation of China (U1704185) and the Science and Technology Opening and Co-production Project of Henan Province of China (182106000060).

References

[1] S.M. Westaway, The potential of transient receptor potential vanilloid type 1 channel modulators for the treatment of pain, Journal of Medicinal Chemistry, 50 (2007) 2589-2596.

[2] A. Szallasi, D.N. Cortright, C.A. Blum, S.R. Eid, The vanilloid receptor TRPV1: 10 years from channel cloning to antagonist proof-of-concept, Nature Reviews Drug Discovery, 6 (2007) 357-372.

[3] L.M. Broad, S.J. Keding, B. Maria-Jesus, Recent progress in the development of selective TRPV1 antagonists for pain, Current Topics in Medicinal Chemistry, 8 (2008) 1431-1441.

[4] N. Khairatkar-Joshi, A. Szallasi, TRPV1 antagonists: the challenges for therapeutic targeting, Trends in Molecular Medicine, 15 (2009) 14-22.

[5] J. Luo, E.T. Walters, S.M. Carlton, H. Hu, Targeting Pain-evoking Transient Receptor Potential Channels for the Treatment of Pain, Current Neuropharmacology, 11 (2013) 652-663.

[6] M. Aghazadeh Tabrizi, P.G. Baraldi, S. Baraldi, S. Gessi, S. Merighi, P.A. Borea, Medicinal Chemistry, Pharmacology, and Clinical Implications of TRPV1 Receptor Antagonists, Medicinal Research Reviews, 37 (2017) 936-983.

[7] J.D. Brederson, P.R. Kym, A. Szallasi, Targeting TRP channels for pain relief, European Journal of Pharmacology, 716 (2013) 61-76.

[8] L. De Petrocellis, A.S. Moriello, Modulation of the TRPV1 channel: current clinical trials and recent

patents with focus on neurological conditions, Recent Patents on Cns Drug Discovery, 8 (2013) 180-204.

[9] G.Y. Wong, N.R. Gavva, Therapeutic potential of vanilloid receptor TRPV1 agonists and antagonists as analgesics: Recent advances and setbacks, Brain Research Reviews, 60 (2009) 267-277.

[10] N.R. Gavva, J.J. Treanor, A. Garami, L. Fang, S. Surapaneni, A. Akrami, F. Alvarez, A. Bak, M. Darling, A. Gore, Pharmacological blockade of the vanilloid receptor TRPV1 elicits marked hyperthermia in humans, Pain, 136 (2008) 202-210.

[11] Y. Lee, S. Hong, M. Cui, P.K. Sharma, J. Lee, S. Choi, Transient receptor potential vanilloid type 1 antagonists: a patent review (2011 - 2014), Expert Opinion on Therapeutic Patents, 25 (2015) 291-318.

[12] M.E. Kort, P.R. Kym, TRPV1 antagonists: clinical setbacks and prospects for future development, Progress in Medicinal Chemistry, 51 (2012) 57-70.

[13] R.M. Reilly, H.A. Mcdonald, P.S. Puttfarcken, S.K. Joshi, L. Lageisha, P. Madhavi, P.H. Franklin, J.A. Segreti, T.R. Neelands, H. Ping, Pharmacology of modality-specific transient receptor potential vanilloid-1 antagonists that do not alter body temperature, Journal of Pharmacology & Experimental Therapeutics, 342 (2012) 416-428.

[14] A. Garami, Y.P. Shimansky, E. Pakai, D.L. Oliveira, N.R. Gavva, A.A. Romanovsky, Contributions of different modes of TRPV1 activation to TRPV1 antagonist-induced hyperthermia, The Journal of Neuroscience, 30 (2010) 1435-1440.

[15] E.A. Voight, A.R. Gomtsyan, J.F. Daanen, R.J. Perner, R.G. Schmidt, E.K. Bayburt, S. DiDomenico, H.A. McDonald, P.S. Puttfarcken, J. Chen, T.R. Neelands, B.R. Bianchi, P. Han, R.M. Reilly, P.H. Franklin, J.A. Segreti, R.A. Nelson, Z. Su, A.J. King, J.S. Polakowski, S.J. Baker, D.M. Gauvin, L.R. Lewis, J.P. Mikusa, S.K. Joshi, C.R. Faltynek, P.R. Kym, M.E. Kort, Discovery of (R)-1-(7-chloro-2,2-bis(fluoromethyl)chroman-4-yl)-3-(3-methylisoquinolin-5-yl)ur ea (A-1165442): a temperature-neutral transient receptor potential vanilloid-1 (TRPV1) antagonist with analgesic efficacy, Journal of Medicinal Chemistry, 57 (2014) 7412-7424.

[16] J. Szychowski, J.F. Truchon, Y.L. Bennani, Natural products in medicine: transformational outcome of synthetic chemistry, Journal of Medicinal Chemistry, 57 (2014) 9292-9308.

[17] S. Wang, S. Yamamoto, Y. Kogure, W. Zhang, K. Noguchi, Y. Dai, Partial Activation and Inhibition of TRPV1 Channels by Evodiamine and Rutaecarpine, Two Major Components of the Fruits of Evodia rutaecarpa, Journal of Natural Products, 79 (2016) 1225-1230.

[18] T. Yuko, H. Syunji, T. Hiromitsu, U. Kunitoshi, T. Makoto, W. Tatsuo, Activation and inhibition of thermosensitive TRP channels by voacangine, an alkaloid present in Voacanga africana, an African tree, Journal of Natural Products, 77 (2012) 285-297.

[19] P. Thirumurugan, D. Matosiuk, K. Jozwiak, Click chemistry for drug development and diverse chemical-biology applications, Chemical Reviews, 113 (2013) 4905-4979.

[20] Y. Gao, E. Cao, D. Julius, Y. Cheng, TRPV1 structures in nanodiscs reveal mechanisms of ligand and lipid action, Nature, 534 (2016) 347-351.

[21] E.L. Poul, S. Hisada, Y. Mizuguchi, V.J. Dupriez, E. Burgeon, M. Detheux, Adaptation of Aequorin Functional Assay to High Throughput Screening, Journal of Biomolecular Screening, 7 (2002) 57.

[22] S.G. Lehto, R. Tamir, H. Deng, L. Klionsky, R. Kuang, A. Le, D. Lee, J.C. Louis, E. Magal, B.H. Manning, Antihyperalgesic effects of (R,E)-N-(2-hydroxy-2,3-dihydro-1H-inden-4-yl)-3-(2-(piperidin-1-yl)-4-(trifluoromethyl)phenyl)-acrylamide (AMG8562), a novel transient receptor potential vanilloid type 1 modulator that does not cause hyperthermia in rats, Journal of Pharmacology & Experimental Therapeutics, 326 (2008) 218-229.

[23] T. Sakurada, A. Sugiyama, C. Sakurada, K. Tanno, A. Yonezawa, S. Sakurada, K. Kisara, Effect of spinal

nitric oxide inhibition on capsaicin-induced nociceptive response, Life Sciences, 59 (1996) 921-930.

[24] T. Lei, C. Yan, C. Zili, P.M. Blumberg, A.P. Kozikowski, W. Zaijie Jim, Antinociceptive pharmacology of N-(4-chlorobenzyl)-N'-(4-hydroxy-3-iodo-5-methoxybenzyl) thiourea, a high-affinity competitive antagonist of the transient receptor potential vanilloid 1 receptor, Journal of Pharmacology & Experimental Therapeutics, 321 (2007) 791-798.

Highlights

• Design, synthesis, and pharmacologic evaluation of a class of TRPV1 antagonists which constructed on 2,3,4,9-tetrahydro-1*H*-pyrido[3,4-b]indole as A-region and triazole as B-region.

• Optimization of this design led to the eventual identification of 2-((1-(2-(trifluoromethyl)phenyl)-1*H*-1,2,3-triazol-4-yl)methyl)-2,3,4,9-tetrahydro-1*H*-pyrido[3,4-b]indole (**6g**), a potent TRPV1 antagonist.

• **6g** exhibited potent antagonism activated by capsaicin (IC_{50} = 0.075 μM) and only partially blocked acid activation of TRPV1, and demonstrated good efficacy in different pain models and did not elevate core body temperature.